GRAVITY PROFILE OVER A BURIED VALLEY IN NORTHEASTERN KANSAS

By Franz Heider

July 1982

University of Kansas

Prepared for Master's Research

Physics Department Course Number 809

Instructor - Dr. H. Yarger

Kansas Geological Survey Open-File Report 82-17

Kansas Geological Survey
Open-file Report

Disclaimer

The Kansas Geological Survey does not guarantee this document to be free from errors or inaccuracies and disclaims any responsibility or liability for interpretations based on data used in the production of this document or decisions based thereon. This report is intended to make results of research available at the earliest possible date, but is not intended to constitute final or formal publication.

Abstract

Gravity data were taken across a buried valley. After the free air-, Bouguer-, tidal- and meter drift-corrections were done, the regional gravity trend is subtracted. The resulting gravity anomaly reflects the bedrock topography. The application of a modeling program restricts the fill material density and the shape of the buried valley to a certain range. Therefore, the gravity method is a useful tool to detect buried bedrock valleys, which are 150 feet deep, or deeper.

INTRODUCTION

In formerly glaciated areas, glacial sediments are often a good source of potable ground water. Northeastern Kansas was glaciated during pre-Illinoian time. The extent of glaciation can be seen on the generalized physiographic map of Kansas (Fig. 1). Also shown is the gravity test site, located in Jefferson county.

Usually bedrock formations contain little high quality water in this area, but large quantities of fresh water may be obtained from glacial buried valley deposits. The buried valleys contain sand and gravel that was deposited by rivers or melt-water streams that flowed in the valleys. The buried valleys often also have till deposits from the glacial ice that overrode the channels. (Personal communication with Jane Denne, 1982).

Normally these buried valleys cannot be recognized at the surface and must therefore be detected by subsurface exploration, either through drilling or geophysical exploration (A. Ibrahim and W.J. Hinze, 1972). Because drilling is slow and expensive, geophysical exploration methods are very useful for the detection of buried channels. These methods consist of remote sensing, temperature profiling, seismic and resistivity methods and the gravity method, which is treated in this paper. The reason why this area was chosen and a description of the other geophysical exploration methods can be found in a paper called "An Integrated Approach for Locating Glacial Buried Valley Aquifers" (Denne and others, 1982).

The gravity data were taken on the 2nd and 9th of September 1980 in an area one mile west of Perry Lake and two miles southwest of the village of Ozawkie. The two lines along which the data were measured can be seen in Figure 2.

The data were measured with a La Coste and Romberg Model G Geodetic gravity meter, which has a reading accuracy of ±0.01 mgal, and a drift rate of less than 1 mgal per month. The meter has a constant temperature bath. The gravity measurement was sensitive to an anomaly, because of the accuracy in measuring the elevation, which was surveyed to 1/100 of a foot, proceeding from the northeast corner of section 3 (mapped elevation 956 ft) south to profile and then west to NWNE section 3 (mapped elevation 988 ft).

GENERALIZED PHYSIOGRAPHIC MAP OF KANSAS

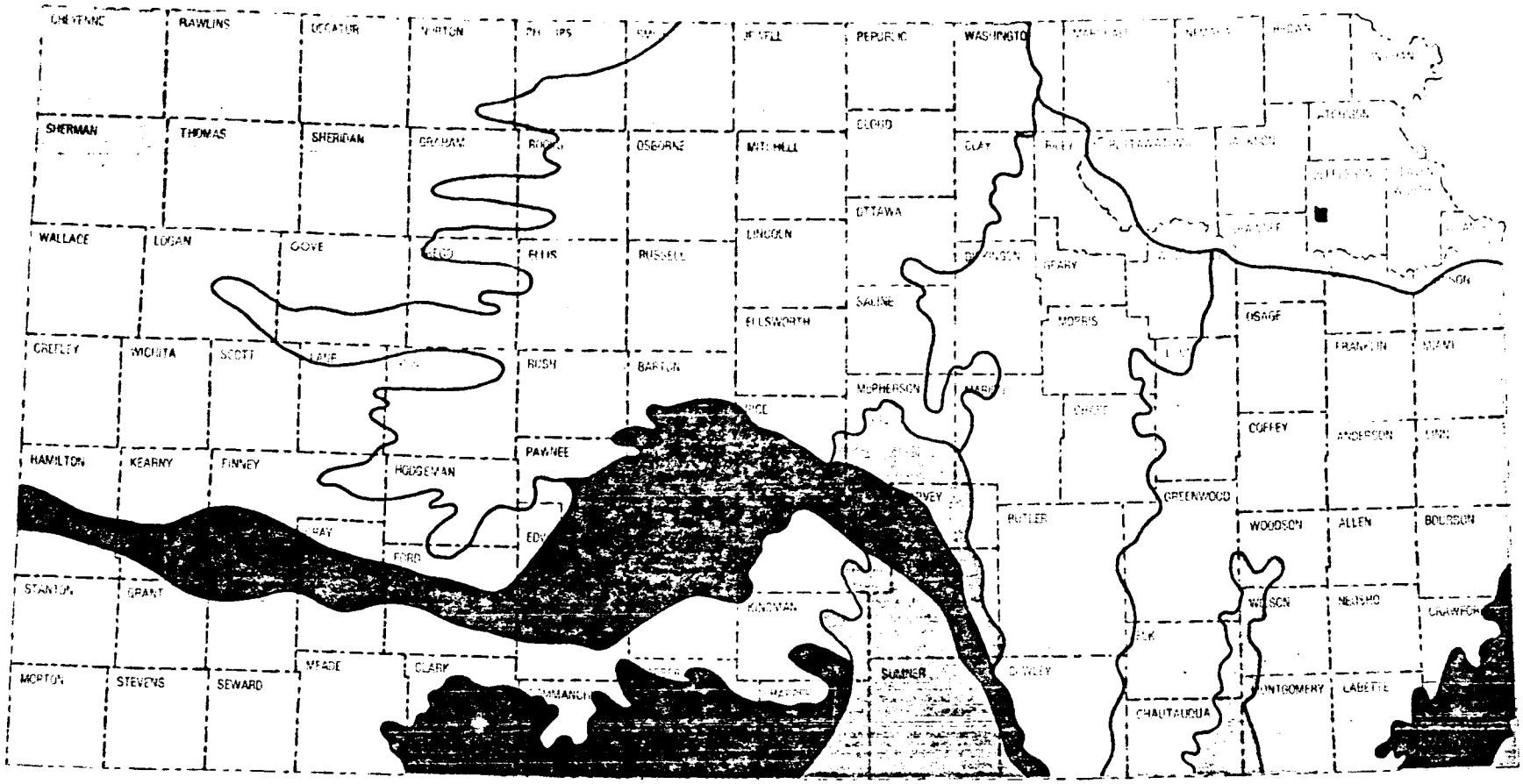

EXPLANATION

■ Area where profile is located

- HIGH PLAINS
- SMOKY HILLS
- ARKANSAS RIVER LOWLANDS
- WELLINGTON-MCPHERSON LOWLANDS
- RED HILLS
- GLACIATED REGION
- OSAGE CUESTAS
- FLINT HILLS UPLANDS
- OZARK PLATEAU
- CHEROKEE LOWLANDS
- CHAUTAUQUA HILLS

0 50 100 miles

0 75 150 kilometers

Fig. 1

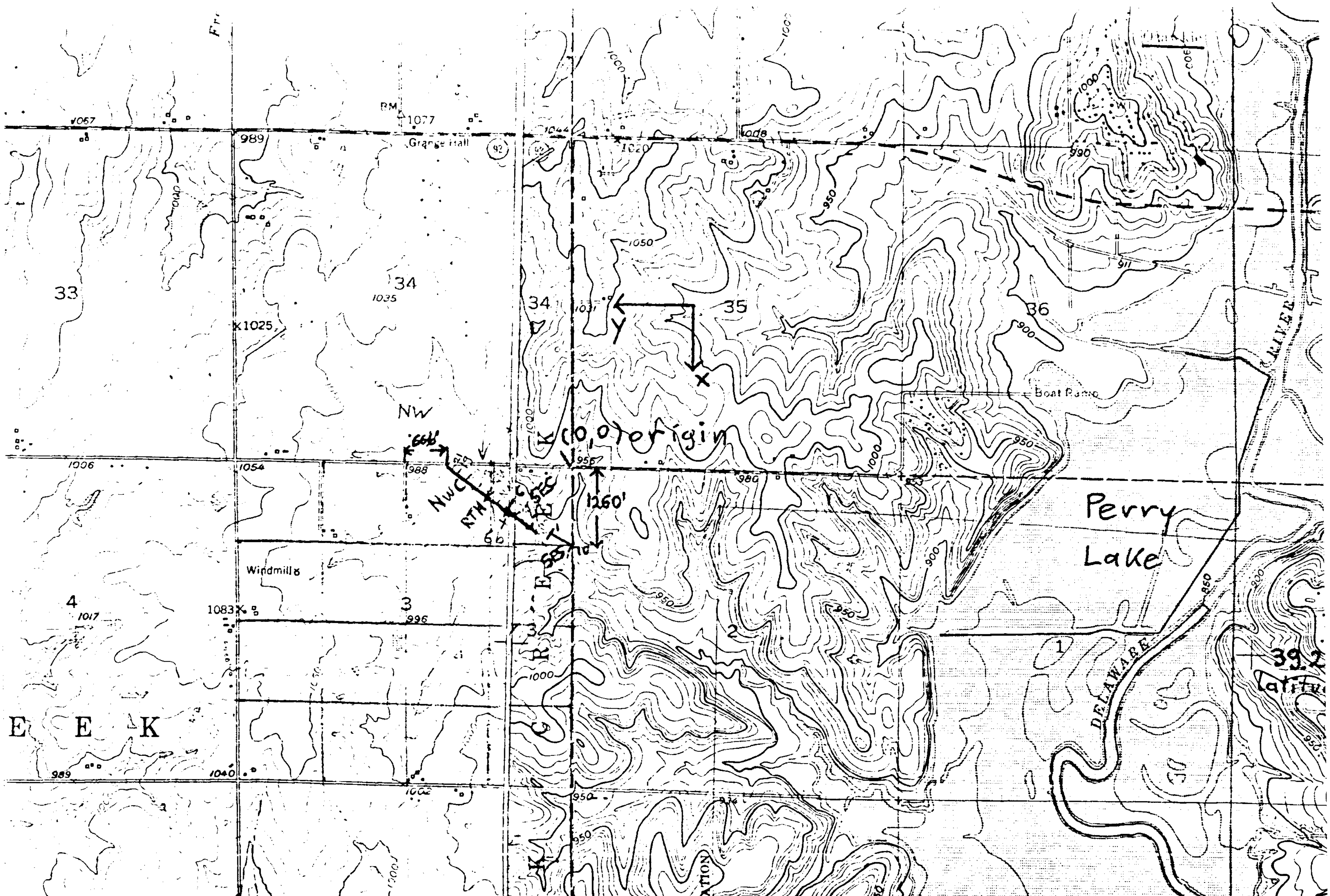

264.5° longitude

264.5' 416

Fig 2

area where data were taken

Gravity Method

The gravity method to locate buried channels was already used by Hall and Hajnal in 1962 to define the configuration of the bedrock surface, particularly where some geological control was available. For a gravity meter with sensitivity of 0.01 mgal, buried valley anomalies greater than about 0.14 mgal can be resolved. This requires that elevations be accurate to ±2 inches. For a drift/bedrock density contrast of 0.3 g/cm^3, valley depths greater than 45 feet can be identified (R.S. Carmichael and G. Henry, Jr., 1977). Generally, bedrock formations are denser than overlying glacial sediments. Therefore, a depression in the bedrock surface, which is filled with sediments, causes a gravity low in comparison to a flat bedrock topography. The correlation between bedrock topography and gravity permits mapping of the subsurface bedrock topography.

From previous non-gravity research there existed a knowledge of the direction and location of the buried valley. The gravity data were therefore taken by another graduate student perpendicular to the valley axis over a distance of 2300 ft.

After having done all the necessary reductions of the data, including free air-, Bouguer-, tidal- and meter drift-correction and after subtracting the regional effect, we expect to see a gravity anomaly in the range of zero to one mgal above the channel due to the density contrast between the valley fill material and the bedrock.

When the topography is relatively flat, like in this case, the above mentioned data reductions provide a sufficiently accurate method of reducing the data to sea level. "If there are considerable irregularities of elevation, particularly in the vicinity of the station, then

the simple assumption that there is an infinite slab of rock between the observation point and sea level is inadequate and a further allowance must be made for departures from this. This is done by computing graphically the gravity effect at the observation point of all hills above the station level and all valleys below it (terrain correction). A method of doing this which is often used is described by Hammer (1939)". (Griffiths, 1976).

In some cases, however, buried bedrock channels are difficult or impossible to delineate by the gravity method because the density of the glacial deposits is nearly equal to that of the adjacent bedrock. In this paper, the gravity data is combined with the information that is available from two drill holes on the profile and others in the region, and these set boundary conditions for the free parameters of width, depth and fill material-density of the valley.

In order to get the final anomaly profile the data had to be processed with the use of several programs, which were changed for this purpose or which were written specifically for this analysis. The former programs were written for bigger areas, for different coordinate systems and for other data-formats. The scale of the coordinate axis had to be changed. For the x-y coordinate system another formula was used to calculate longitude and latitude. The Fortran programs were run on the Honeywell computer.

Coordinate system:

Before feeding the data into the first program, a coordinate system for the data points had to be established. As origin, the crossing

of the two roads which meet northeast of the data line was chosen. (See Fig. 2).

By knowing the x- and y-coordinates of the base station SES(South-East-South)10 the coordinates of the points SES9 to SES1 are easily calculated. The necessary information, including angle of the data line towards north and distances between the single points, were measured in the field and given in the report.

Fig. 3:

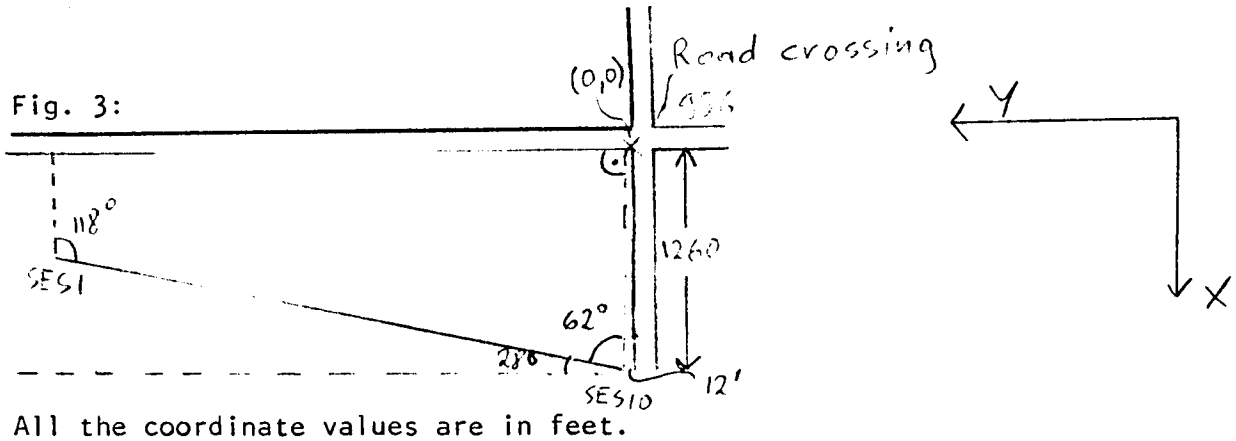

All the coordinate values are in feet.

To get the linear equation for the line SES(1-10), its slope and intersection with the y-axis have to be determined.

Slope a of line SES(1-10):

$$a = \tan 62^{\circ} = 1.88073$$

Intersection b with the y-axis:

$$b = 1.88073 * 1260 = 2369.72$$

Linear equation for line SES(1-10):

$$y = a * x + b$$

$$y = 1.8807 * x + 2369.7$$

The coordinates of the base station SES10 are:

$$x = 1260 \quad y = -2$$

By knowing the distance d between the points SES(9-1) the x- and y-values are obtained from:

$$x = 1260 - d * \sin 28^{\circ}$$

$$y = -2 + d * \cos 28^{\circ}$$

Fig. 4:

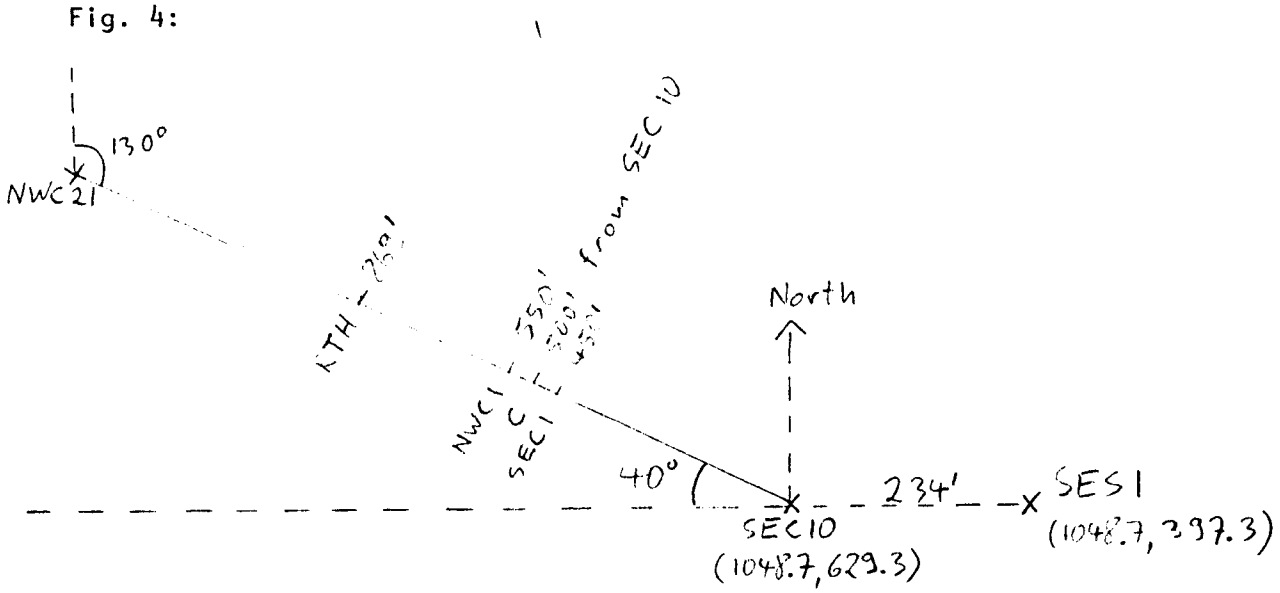

Similarly, the x- and y-coordinates for the remaining points SEC10 to NWC21 were determined from:

$$x = 1048.7 - d * \sin 40^{\circ}$$

$$y = 629.3 + d * \cos 40^{\circ}$$

Program INITIAL

The first program INITIAL reads in coordinates x, y, elevation z, time, date, gravity meter reading and station name. The x- and y-coordinates were necessary to calculate the longitude Beta and latitude Phi of the data locations. Beta and Phi are needed in a subroutine called TIDE, which calculates the tidal attraction of sun and moon at a certain time, at a certain place.

Another subroutine called GCNVERT converts the meter reading from the field into a raw gravity value, which is in milligals.

INITIAL lists the following data in table form: (Fig. 5a and 5b)

- The data that were read in
- RAW G, which is the converted meter reading in milligals
- G SUB R, is the gravity of a spheroid, calculated by use of the International Gravity Formula:

$$g_r = 978031.85*(0.000023462*\sin^4(Phi) + 0.005278895*\sin^2(Phi) + 1)$$

where Phi is the geographic latitude. This formula considers, that the gravity at sea level varies smoothly from the equator to the poles.

- BOUGUER is the Bouguer gravity value, which will be explained later.

PROFILE plots two graphs:

1. The tidal effect at the base station (Fig. 6a and 6b)
2. The Bouguer gravity versus tie line (Fig. 7)

Data from the first day

BASE IS 1260.0 , Y BASE IS -2.0 , DATE: [illegible] , METER NO. 4 , OPERATOR 4

X	Y	Z(FT)	TIME	METER	RAW G	G SUB B	BOUGUER	TIDE	COMMENTS
1260.0	-2.0	930.10	3:50P	3500.579	3652.244	980099.0161	-976391.005	0.0488	SES10
1236.5	42.1	928.09	3:56P	3500.738	3652.411	980099.0219	-976391.068	0.	SES9
1213.1	86.3	928.70	4: 0P	3500.683	3652.354	980099.0275	-976390.994	0.	SES8
1189.6	130.4	929.23	4: 7P	3500.648	3652.317	980099.0333	-976391.005	0.	SES7
1166.1	174.6	929.78	4:12P	3500.583	3652.229	980099.0390	-976391.060	0.	SES6
1142.6	218.7	930.76	4:17P	3500.540	3652.234	980099.0447	-976391.037	0.	SES5
1119.2	262.9	932.10	4:22P	3500.525	3652.189	980099.0504	-976391.078	0.	SES4
1095.7	307.0	932.24	4:26P	3500.498	3652.152	980099.0561	-976391.082	0.	SES3
1072.2	351.2	932.20	4:33P	3500.487	3652.148	980099.0618	-976391.024	0.	SES2
1048.7	395.3	931.88	4:37P	3500.486	3652.147	980099.0675	-976391.051	0.	SES1
1048.7	629.3	930.52	5: 2P	3500.576	3652.240	980099.0675	-976391.037	0.	SEC10
1016.6	667.6	931.48	5: 7P	3500.565	3652.231	980099.0753	-976390.999	0.	SEC9
984.4	705.9	932.69	5:14P	3500.385	3652.042	980099.0831	-976391.122	0.	SEC8
952.3	744.2	933.72	5:19P	3500.397	3652.055	980099.0909	-976391.054	0.	SEC7
920.1	782.5	934.97	5:25P	3500.337	3651.992	980099.0988	-976391.051	0.	SEC6
855.9	859.1	937.32	5:39P	3500.013	3651.654	980099.1144	-976391.268	0.	SEC4
791.6	935.7	939.80	5:42P	3499.791	3651.423	980099.1300	-976391.363	0.	SEC2
759.4	974.0	940.88	5:47P	3499.686	3651.307	980099.1378	-976391.422	0.	SEC1
823.7	897.4	938.36	5:57P	3500.000	3651.640	980099.1222	-976391.227	0.	SEC3
887.3	920.8	936.13	6: 1P	3500.142	3651.804	980099.1168	-976391.173	0.	SEC5
727.3	1012.3	941.35	6: 7P	3499.630	3651.254	980099.1457	-976391.453	0.	C
695.2	1050.6	941.42	6:11P	3499.570	3651.192	980099.1535	-976391.520	0.	NWC1
663.0	1088.9	941.70	6:18P	3499.598	3651.221	980099.1613	-976391.482	0.	NWC2
630.9	1127.2	942.48	6:22P	3499.500	3651.119	980099.1691	-976391.545	0.	NWC3
566.6	1203.8	943.37	6:26P	3499.535	3651.155	980099.1847	-976391.471	0.	NWC5
598.7	1165.5	942.76	6:30P	3499.550	3651.171	980099.1769	-976391.484	0.	NWC4
534.5	1242.1	943.82	6:33P	3499.610	3651.233	980099.1925	-976391.373	0.	NWC6
502.3	1280.4	945.28	6:37P	3499.600	3651.223	980099.2004	-976391.384	0.	NWC7
490.1	1295.0	945.58	6:40P	3499.509	3651.128	980099.2033	-976391.384	0.	RTH
1260.0	-2.0	930.10	6:46P	3500.540	3652.204	980099.0161	-976391.048	0.0384	SES10

Fig 5a

Data from the second day

X BASE IS 1260.0 , Y BASE IS -2.0 , DATE: 9- 9-80 , METER NO. 4 , OPERATOR 4

X	Y	Z(FT)	TIME	METER	RAW G	G SUB R	BOUGUER	TIDE	COMMENTS
1260.0	-2.0	930.10	3:24P	3500.348	3652.004	980099.0161	-976391.249	0.0562	SES10
438.0	1357.0	947.92	3:35P	3499.400	3651.014	980099.2160	-976391.370	0.	NWC9
405.9	1395.3	948.47	4: 2P	3499.392	3651.006	980099.2238	-976391.353	0.	NWC10
373.8	1433.6	948.97	4:10P	3499.396	3651.010	980099.2316	-976391.327	0.	NWC11
341.6	1471.9	949.67	4:21P	3499.501	3651.120	980099.2394	-976391.183	0.	NWC12
309.5	1510.3	950.41	4:38P	3499.502	3651.121	980099.2472	-976391.146	0.	NWC13
277.4	1548.6	951.83	4:47P	3499.453	3651.069	980099.2550	-976391.119	0.	NWC14
245.2	1586.9	952.62	4:54P	3499.410	3651.024	980099.2629	-976391.126	0.	NWC15
1260.0	-2.0	930.10	5: 6P	3500.522	3652.186	980099.0161	-976391.067	0.0862	SES10
180.9	1663.5	953.86	5:14P	3499.366	3650.978	980099.2785	-976391.112	0.	NWC16
148.8	1701.8	953.94	5:13P	3499.431	3651.046	980099.2863	-976391.047	0.	NWC17
116.7	1740.1	954.79	5:24P	3499.397	3651.011	980099.2941	-976391.040	0.	NWC18
84.5	1778.4	956.18	5:30P	3499.408	3651.022	980099.3019	-976390.953	0.	NWC19
52.4	1816.7	958.67	5:34P	3499.298	3650.907	980099.3097	-976390.926	0.	NWC20
20.2	1855.0	960.37	5:37P	3499.263	3650.871	980099.3176	-976390.869	0.	NWC21
490.1	1295.0	945.58	[illegible]:56P	3499.662	3651.288	980099.2033	-976391.224	0.	RTH
470.2	1318.7	946.60	:56P	3499.602	3651.225	980099.2082	-976391.230	0.	NWC8
0.0	-2.0	930.10	6: 5P	3500.562	3652.227	980099.0161	-976391.025	0.0773	SES10

Fig 5b

GTIDE VS TIME

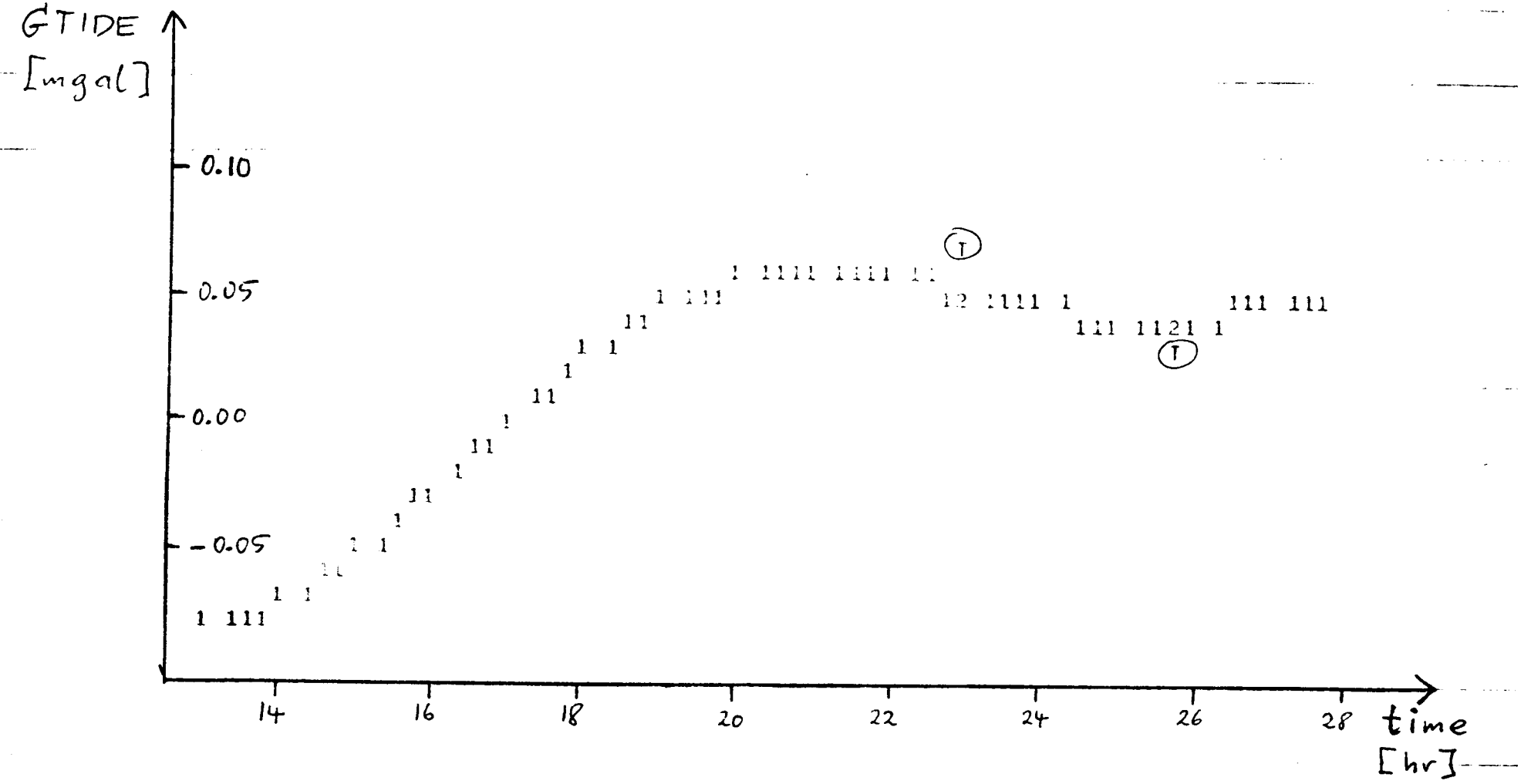

root mean square = 0.015

T is the base station reading

date 9/2/80

Fig 6a

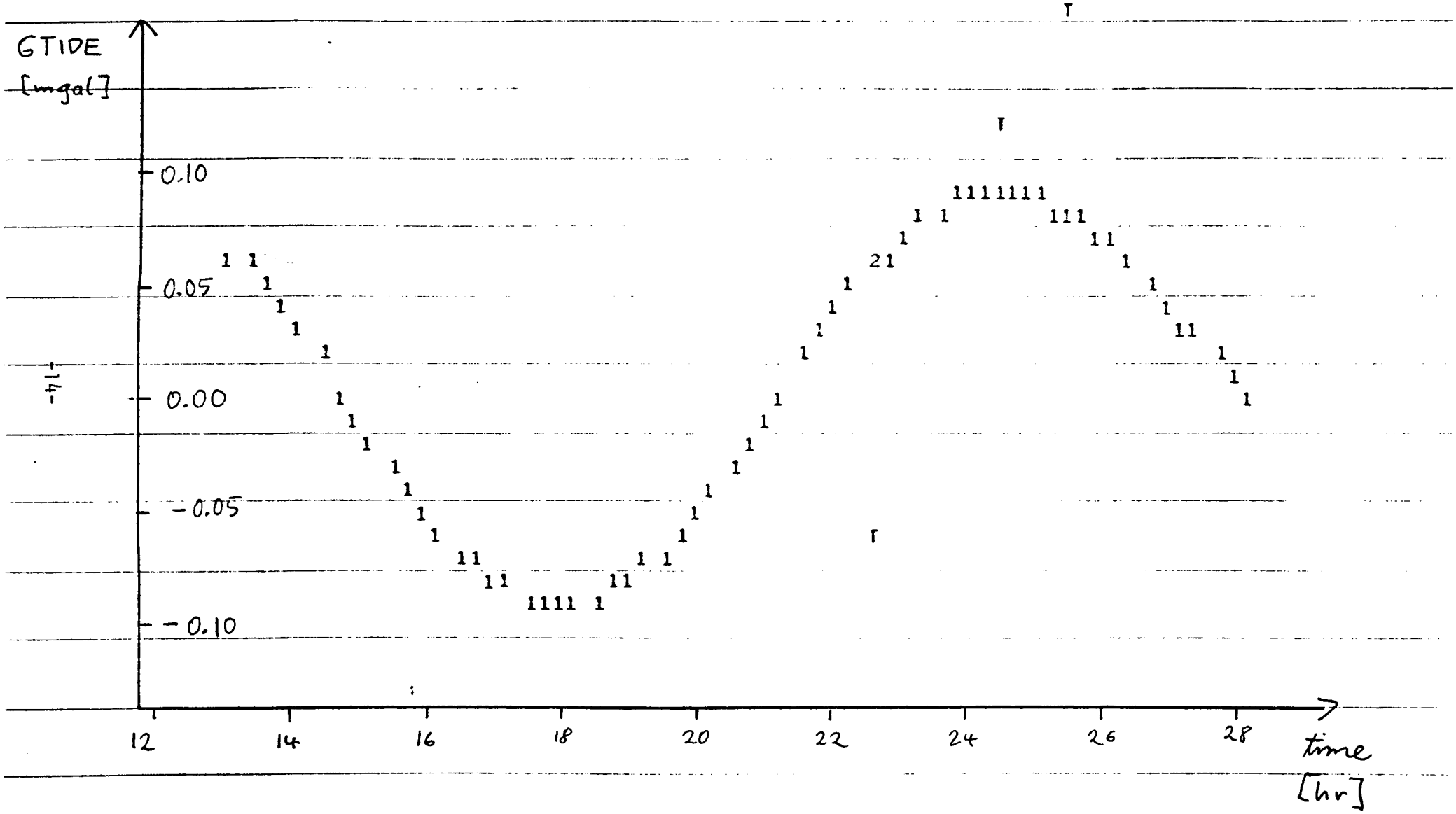

root mean square = 0.086

T is the basestation reading

date 9/9/80

Fig 6b

Bouguer gravity vs y-axis

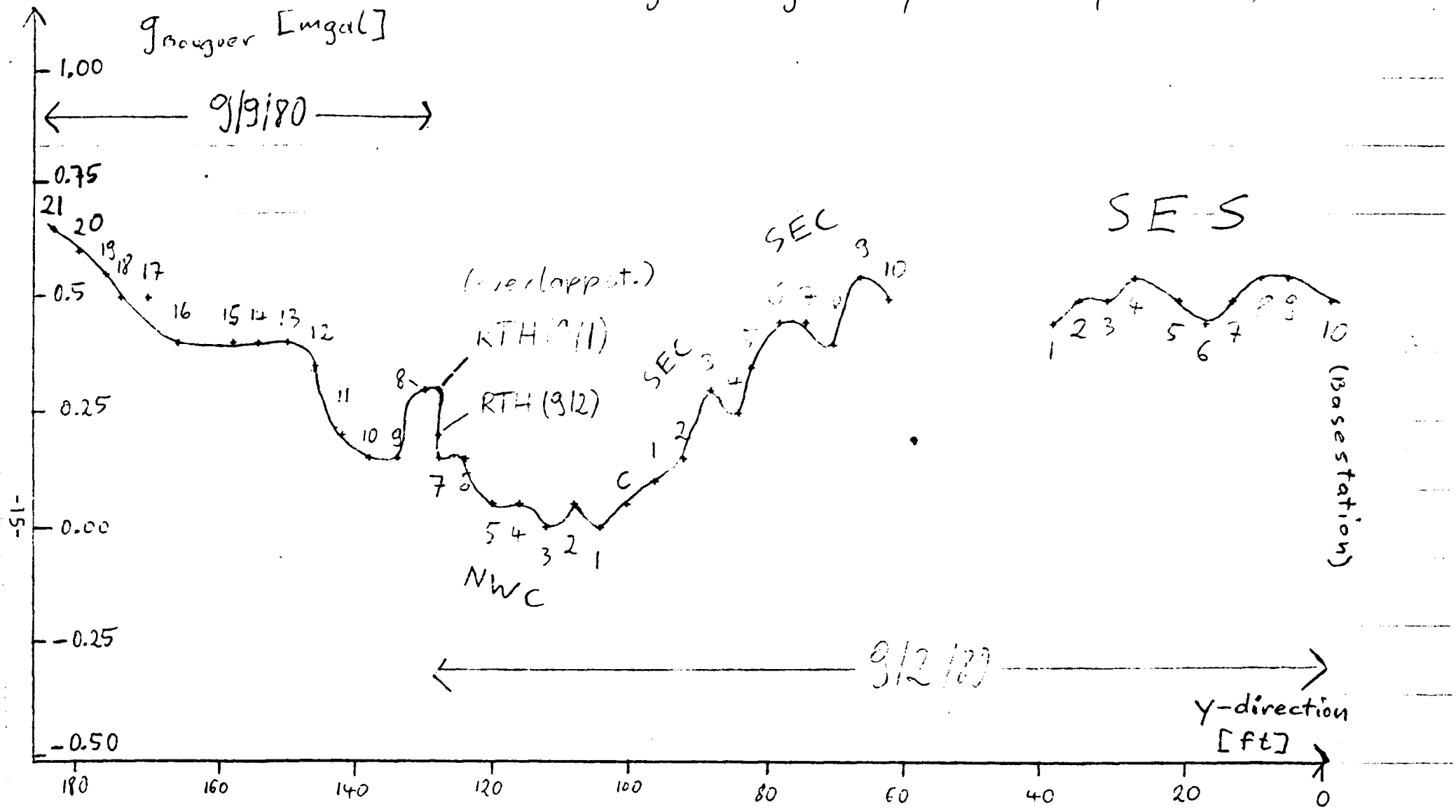

Fig-7

Gravity Tidal Effects

There are external time variations of gravity which result from the variation in the gravitational attraction of the sun and the moon as their positions change with respect to the earth. For certain configurations of the sun and moon, the rotation of the earth produces changes that have a maximum amplitude of about 0.3 mgal and occur in a period as short as about 6 hours. The details of the tidal gravity change vary widely with the different phases of the moon, as indicated by Fig. 8:

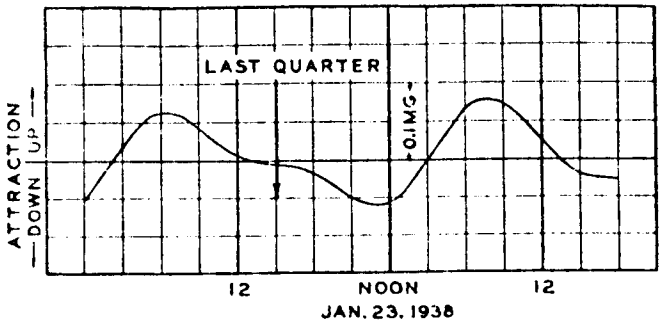

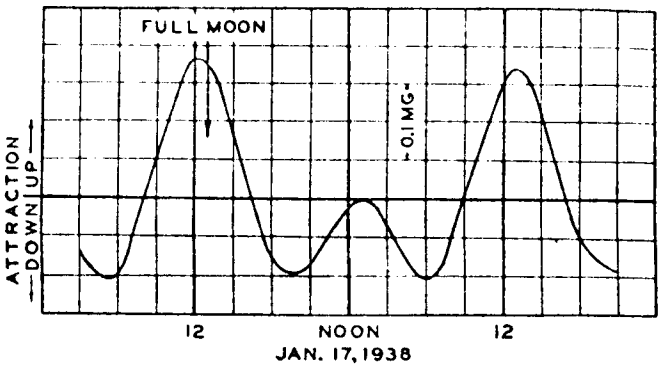

The three measured values at the basestation for 9/9/80 are in relatively poor accordance with the theoretically calculated values (Fig. 6b). The root mean square value = 0.086 milligals which is larger than the meter accuracy but still acceptable for this study. The result of this poor fit is a bigger meter drift for the 9/9/80 than for the 9/2/80. The two measured values at the basestation for 9/2/80 are much closer to the theoretical graph. The root mean square value = 0.015 milligals which is consistent with the meter accuracy (Fig. 6b).

Program SLOPE

Program SLOPE is run after INITIAL and calculates the drift of the gravity meter from the multiple daily readings taken at the base station SES10. All gravity instruments show a small amount of drift, or variation over time due to very small changes in elongation or torsion of the spring system.

To provide data for the drift correction, the gravity meter is returned to a reference station two or three times per day. It is precise enough to make a linear interpolation between drift readings. The meter drift gravity value is obtained by subtracting the tidal gravity effect from the converted meter reading. In this case there were three base station meter readings made on the first day and two on the second day. The following values were printed out by the SLOPE program:

DATE	METERDRIFT Gravity Value G_{md}	JULIAN TIME	SLOPE (milligals/hour)
9/2	3652.19530	0.80672009	-0.009769
9/2	3652.16603	0.80672344	
9/9	3651.94750	0.80691124	0.089343
9/9	3652.09938	0.80691319	0.051542
9/9	3652.15006	0.80691431	

A rough draft of the linear interpretation looks like this: (Fig. 9)

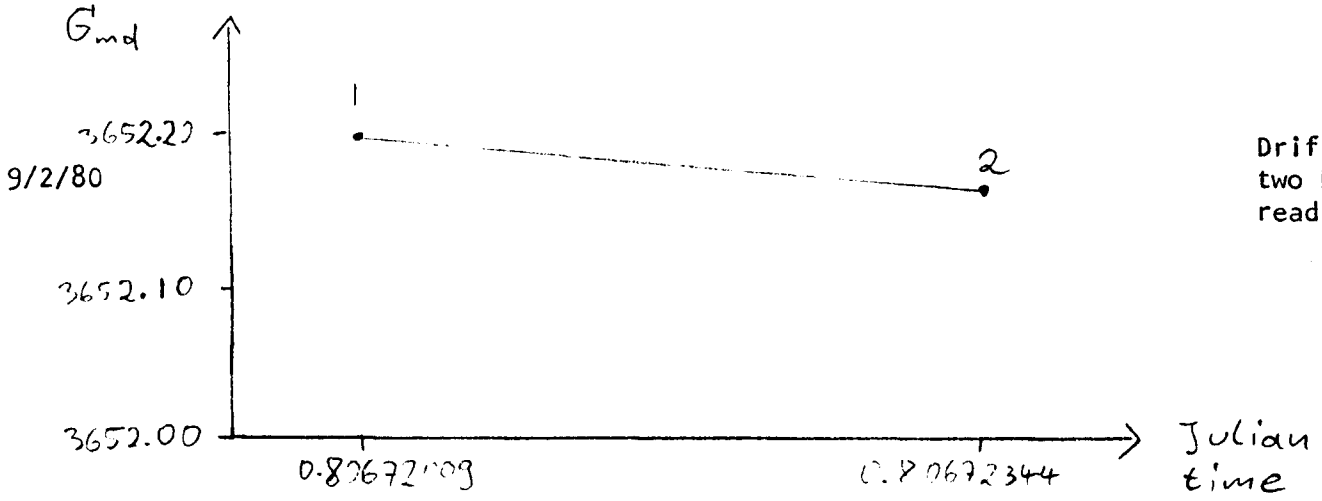

Drift between two base station readings

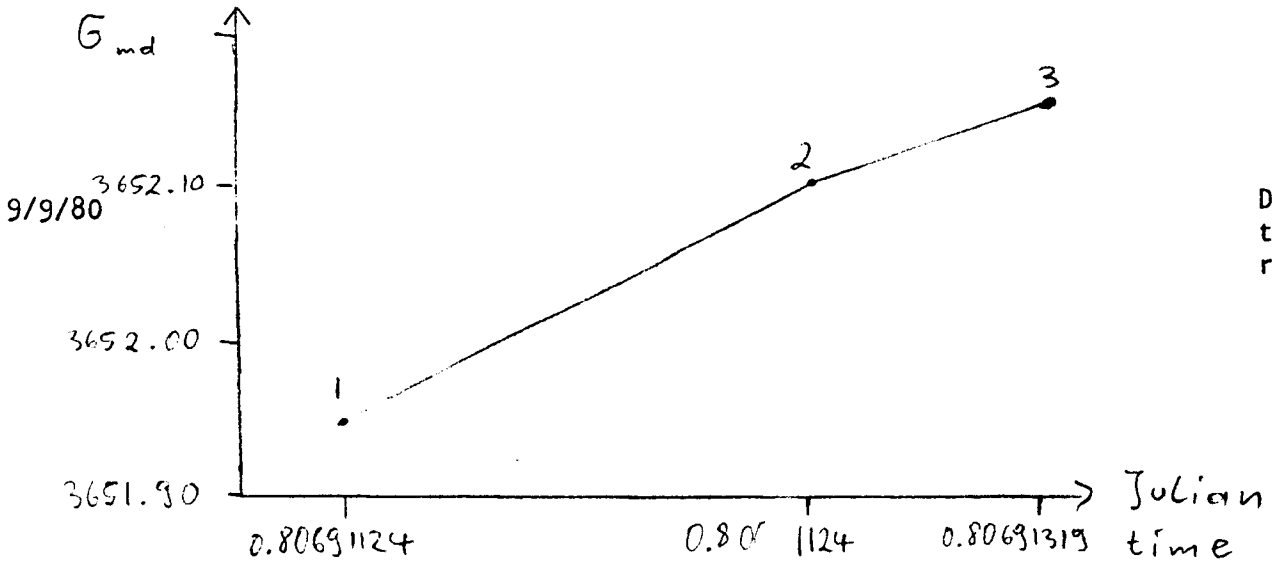

Drift between three basestation readings

As remarked above the theoretically calculated tidal drift value here is already subtracted. Like all the other data, Meter drift, Julian time and Slope also are stored on permanent files to be used again in the next program STATION TIE IN.

Program STATION TIE IN

In this case the base station was not tied in to an absolute gravity value. For the purpose of detecting a buried channel it is sufficient to know relative gravity values. Therefore, the main step in this program is the subtraction of the meter drift (slope) from the tidal corrected gravity values. That means, that from each gravity value there is another amount of drift subtracted according to the time at which the measurement was made. This tidal and meter drift corrected data are printed out and stored with the name SABSGRAV (station absolute gravity), although it is only a relative value. For the following data the base station absolute gravity was arbitrarily taken to be 980000. mgal. Note also that in Fig. 10 the nineteenth and fiftieth data values signal the end of the day for the program. In the next step these data that were stored on a file named TIEDATA (Fig. 10) are read into PROFILE1.

SHOMB = 75951, ACTIVITY # = 029, REPORT CODE = 06, RECORD COUNT = 000050

1260.0	-2.0	930.10	324P	3500.348	B	1260.0	-2.0	9	9	980000.000	980000.00
438.0	1357.0	947.92	335P	3499.400	S	1260.0	-2.0	9	9	980000.000	979998.98
405.9	1395.3	948.47	4 2P	3499.392	S	1260.0	-2.0	9	9	980000.000	979998.92
373.8	1433.6	948.97	410P	3499.396	S	1260.0	-2.0	9	9	980000.000	979998.91
341.6	1471.9	949.67	421P	3499.501	S	1260.0	-2.0	9	9	980000.000	979999.00
309.5	1510.3	950.41	438P	3499.502	S	1260.0	-2.0	9	9	980000.000	979998.97
277.4	1548.6	951.83	447P	3499.453	S	1260.0	-2.0	9	9	980000.000	979998.91
245.2	1586.9	952.62	454P	3499.410	S	1260.0	-2.0	9	9	980000.000	979998.85
1260.0	-2.0	930.10	5 6P	3500.522	B	1260.0	-2.0	9	9	980000.000	980000.00
180.9	1663.5	953.86	514P	3499.366	S	1260.0	-2.0	9	9	980000.000	979998.78
148.8	1701.8	953.94	519P	3499.431	S	1260.0	-2.0	9	9	980000.000	979998.85
116.7	1740.1	954.79	524P	3499.397	S	1260.0	-2.0	9	9	980000.000	979998.81
84.5	1778.4	956.18	530P	3499.408	S	1260.0	-2.0	9	9	980000.000	979998.81
52.4	1816.7	958.67	534P	3499.298	S	1260.0	-2.0	9	9	980000.000	979998.69
20.2	1855.0	960.37	537P	3499.263	S	1260.0	-2.0	9	9	980000.000	979998.66
490.1	1295.0	945.58	546P	3499.662	O	1260.0	-2.0	9	9	980000.000	979999.07
470.2	1318.7	946.60	556P	3499.602	S	1260.0	-2.0	9	9	980000.000	979999.00
1260.0	-2.0	930.10	6 5P	3500.562	B	1260.0	-2.0	9	9	980000.000	980000.00
0.	9999.0	0.	0 0P	0.	S	1260.0	-2.0	0	0	980000.000	980000.00
1260.0	-2.0	930.10	350P	3500.578	B	1260.0	-2.0	9	2	980000.000	980000.00
1236.5	42.1	928.08	356P	3500.738	S	1260.0	-2.0	9	2	980000.000	980000.16
1213.1	86.3	928.70	4 2P	3500.683	S	1260.0	-2.0	9	2	980000.000	980000.11
1189.6	130.4	929.23	4 7P	3500.648	S	1260.0	-2.0	9	2	980000.000	980000.07
1166.1	174.6	929.78	412P	3500.563	S	1260.0	-2.0	9	2	980000.000	979999.99
1142.6	218.7	930.76	417P	3500.540	S	1260.0	-2.0	9	2	980000.000	979999.96
1119.2	262.9	932.10	422P	3500.525	S	1260.0	-2.0	9	2	980000.000	979999.95
1095.7	307.0	932.24	426P	3500.499	S	1260.0	-2.0	9	2	980000.000	979999.92
1072.2	351.2	932.20	433P	3500.487	S	1260.0	-2.0	9	2	980000.000	979999.91
1048.7	395.3	931.88	439P	3500.485	S	1260.0	-2.0	9	2	980000.000	979999.91
1048.7	629.3	930.52	5 2P	3500.576	S	1260.0	-2.0	9	2	980000.000	980000.01
1016.6	667.6	931.48	5 7P	3500.565	S	1260.0	-2.0	9	2	980000.000	980000.00
984.4	705.9	932.69	514P	3500.385	S	1260.0	-2.0	9	2	980000.000	979999.82
952.3	744.2	933.72	519P	3500.397	S	1260.0	-2.0	9	2	980000.000	979999.83
920.1	782.5	934.97	525P	3500.337	S	1260.0	-2.0	9	2	980000.000	979999.77
855.9	859.1	937.32	538P	3500.013	S	1260.0	-2.0	9	2	980000.000	979999.43
791.6	935.7	939.80	542P	3499.791	S	1260.0	-2.0	9	2	980000.000	979999.20
759.4	974.0	940.88	547P	3499.680	S	1260.0	-2.0	9	2	980000.000	979999.09
823.7	897.4	938.30	557P	3500.000	S	1260.0	-2.0	9	2	980000.000	979999.42
887.3	820.8	936.13	6 1P	3500.162	S	1260.0	-2.0	9	2	980000.000	979999.59
727.3	1012.3	941.35	6 7P	3499.630	S	1260.0	-2.0	9	2	980000.000	979999.04
695.2	1050.6	941.42	611P	3499.570	S	1260.0	-2.0	9	2	980000.000	979998.98
663.0	1088.9	941.70	618P	3499.598	S	1260.0	-2.0	9	2	980000.000	979999.01
630.9	1127.2	942.48	622P	3499.500	S	1260.0	-2.0	9	2	980000.000	979998.91
566.6	1203.8	943.37	626P	3499.535	S	1260.0	-2.0	9	2	980000.000	979998.94
598.7	1165.5	942.76	630P	3499.550	S	1260.0	-2.0	9	2	980000.000	979998.96
534.5	1242.1	943.82	633P	3499.610	S	1260.0	-2.0	9	2	980000.000	979999.02
502.3	1280.4	945.29	637P	3499.600	S	1260.0	-2.0	9	2	980000.000	979999.01
490.1	1295.0	945.58	640P	3499.509	O	1260.0	-2.0	9	2	980000.000	979998.92
1260.0	-2.0	930.10	645P	3500.540	B	1260.0	-2.0	9	2	980000.000	980000.00
0.	9999.0	0.	0 0P	0.	S	1260.0	-2.0	0	0	980000.000	980000.00

X Y Z time g, meter reading station X-base Y-base date Babsgrav Sabsgrav

B = Base station

S = station

O = Overlapp station (RTH)

Fig. 10

Program PROFILE1

The purpose of PROFILE1 is to display different aspects of the gravity data.

1) The elevation in meters is plotted versus the distance from the station NWC21. From now on the graphs are not a projection along a certain latitude, but the data are now displayed versus the line along which they were taken. The variable DIST has the units of ft/10. The elevation is somewhat linearly decreasing from 293m to 283m and levels off in the direction of the base station. This plot in Fig. 11 shows two gaps, which represent small creeks between the stations NWC16-NWC15 and SEC10-SES1. The remaining stations are 50 feet apart from each other. The encircled number 2 in the plot is the overlap station RTH and the encircled number 4 is where four base station readings were made.

2) The raw gravity versus distance plot (Fig. 12) does not show the expected gravity anomaly, because it first has to be corrected for the two following effects.

3) The free air effect (Fig. 13) is due to a vertical decrease of gravity with increase of elevation. The reference level is the sea level and the correction must be added to stations at a higher elevation.

The free air anomaly is defined as:

$$\Delta g_{FA} = \text{SABSGRAV} + 0.3086 * \text{ELEVATION}$$

or

$$\Delta g_{FA} = g_{obs} - g_{theor} + C_{FA} * h$$

4) Fig. 14 shows the Bouguer anomaly versus distance (ft/10). It takes the attraction of the material of density 2.0g/cm^3 between the lowest elevation (928.08m) and the elevation of the individual station into account. The correction for the attraction is approximated by an infinite horizontal slab of material of a certain density ρ. As a reasonable value ρ was chosen to be 2.0 g/cm^3. The Bouguer anomaly is defined as:

$$\Delta g_B = \Delta g_{FA} - C_B \rho h$$

There is a significant anomaly in the graph, which can be explained by the lower density fill material of the valley.

5) Fig. 15 shows DELG/FOOT versus distance. It is the change in gravity per foot with error bars S. The main effect if you go to another station is the change in elevation. Therefore, the elevation effect should be a constant. Because the data (T) lie quite well along a line, it can be concluded that the data are accurate.

6) Fig. 16 shows the free air anomaly versus elevation.
In an ideal case the free air gravity could be used for density determination. Starting from the formula

$$\Delta g_{FA} = g_{obs} - g_{theor} + C_{FA} * h$$

where:

Δg_{FA} = free air anomaly

g_{obs} = observed gravity

g_{theor} = theoretically calculated gravity

h = elevation

C_{FA} = free air constant

from the definition of the Bouguer anomaly follows:

$$\Delta g_{FA} = \Delta g_B + h \rho C_B$$

Where

ρ = density

C_B = Bouguer constant

If there were no local anomaly such as the one in this case caused by the buried valley, the Bouguer anomaly Δg_B would be taken constant. Then the linear equation in h could be solved for the density ρ . A try in this case failed because the density values obtained were much too high.

7) Fig. 17 shows a plot of latitude versus longitude. These are the two lines along which the data were taken. It displays a more detailed picture of the data locations from Fig. 2. It also serves as a check for the formulas that determine longitude and latitude.

At the end of PROFILE the distances DIST are printed out. They were calculated from the x, y coordinates of the individual stations and offer, therefore, a check for the correctness of the formulas. Also printed are the Bouguer gravity values from Fig. 14, which are the main data to continue within the next program.

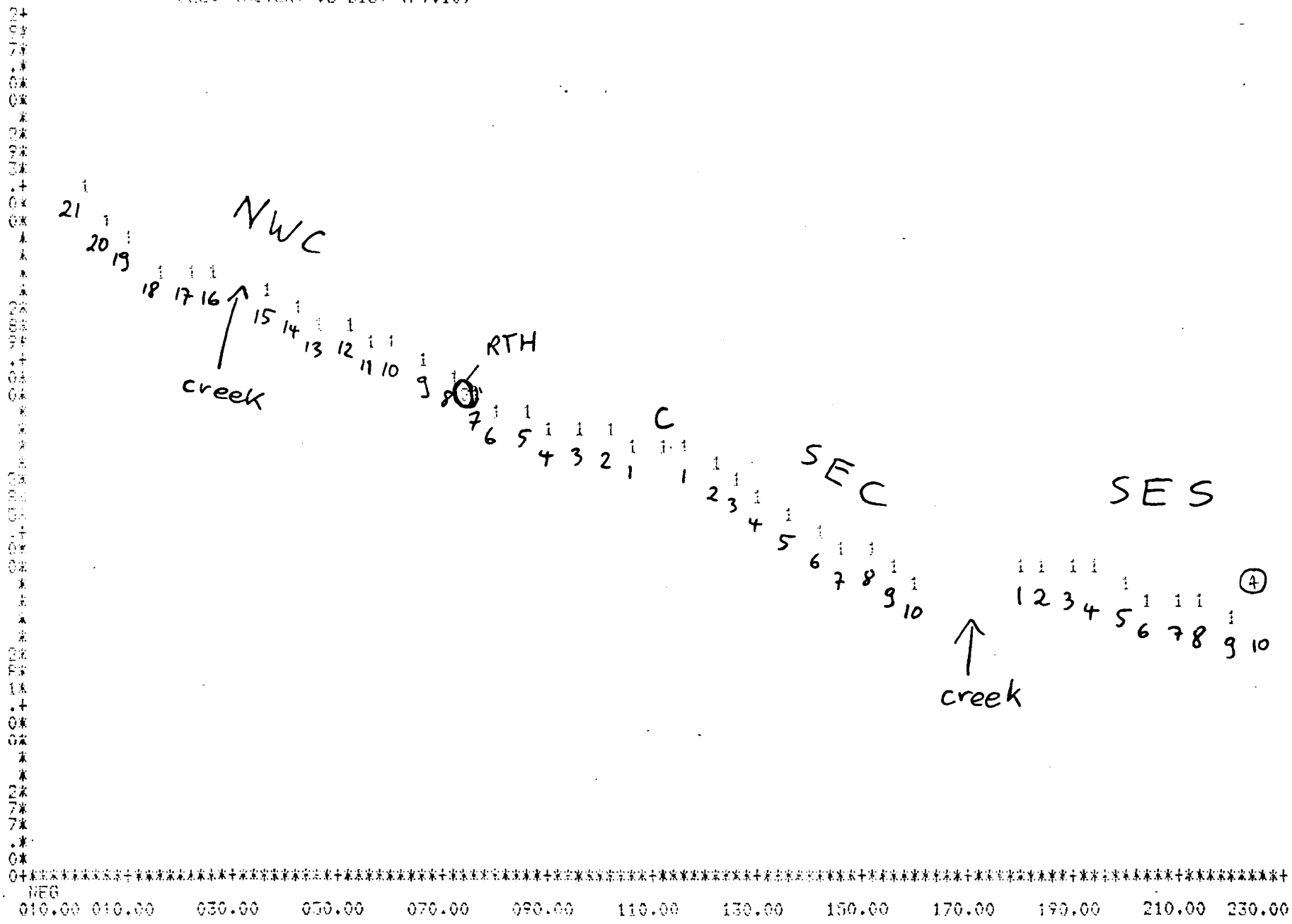
ELEV (METER) VS DIST (FT:10)
NWC
RTH
C
SEC
SES
creek
creek
NEG
010.00 010.00 030.00 050.00 070.00 090.00 110.00 130.00 150.00 170.00 190.00 210.00 230.00

Fig. 11

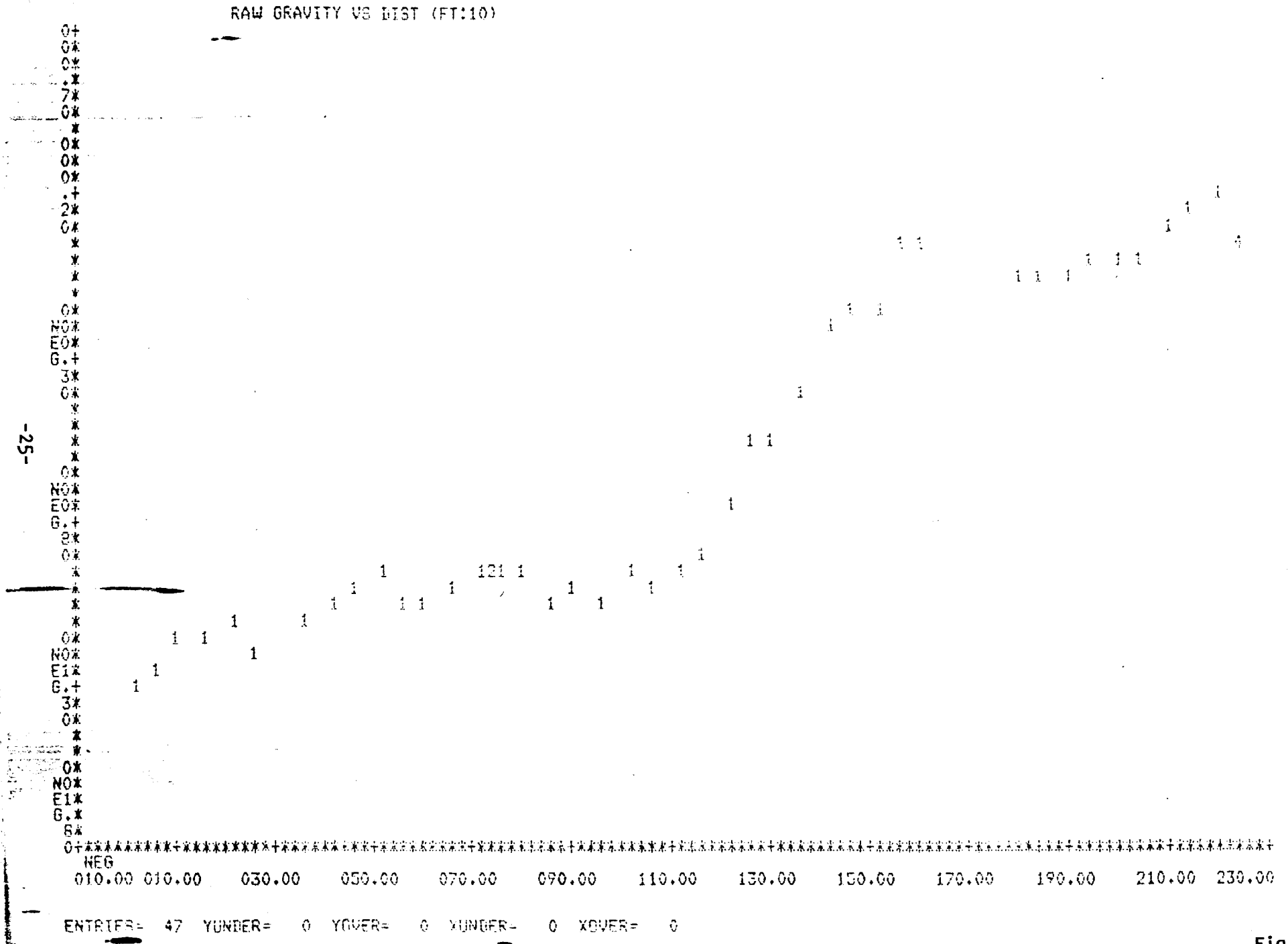
RAW GRAVITY VS DIST (FT:10)
NEG
010.00 010.00 030.00 050.00 070.00 090.00 110.00 130.00 150.00 170.00 190.00 210.00 230.00
ENTRIES= 47 YUNDER= 0 YOVER= 0 XUNDER= 0 XOVER= 0

Fig. 12

010.00 010.00 030.00 050.00 070.00 090.00 110.00 130.00 150.00 170.00 190.00 210.00 230.00

ENTRIES= 47 YUNDER= 0 YOVER= 0 XUNDER= 0 XOVER= 0

FREE AIR VS DIST (FT:10)

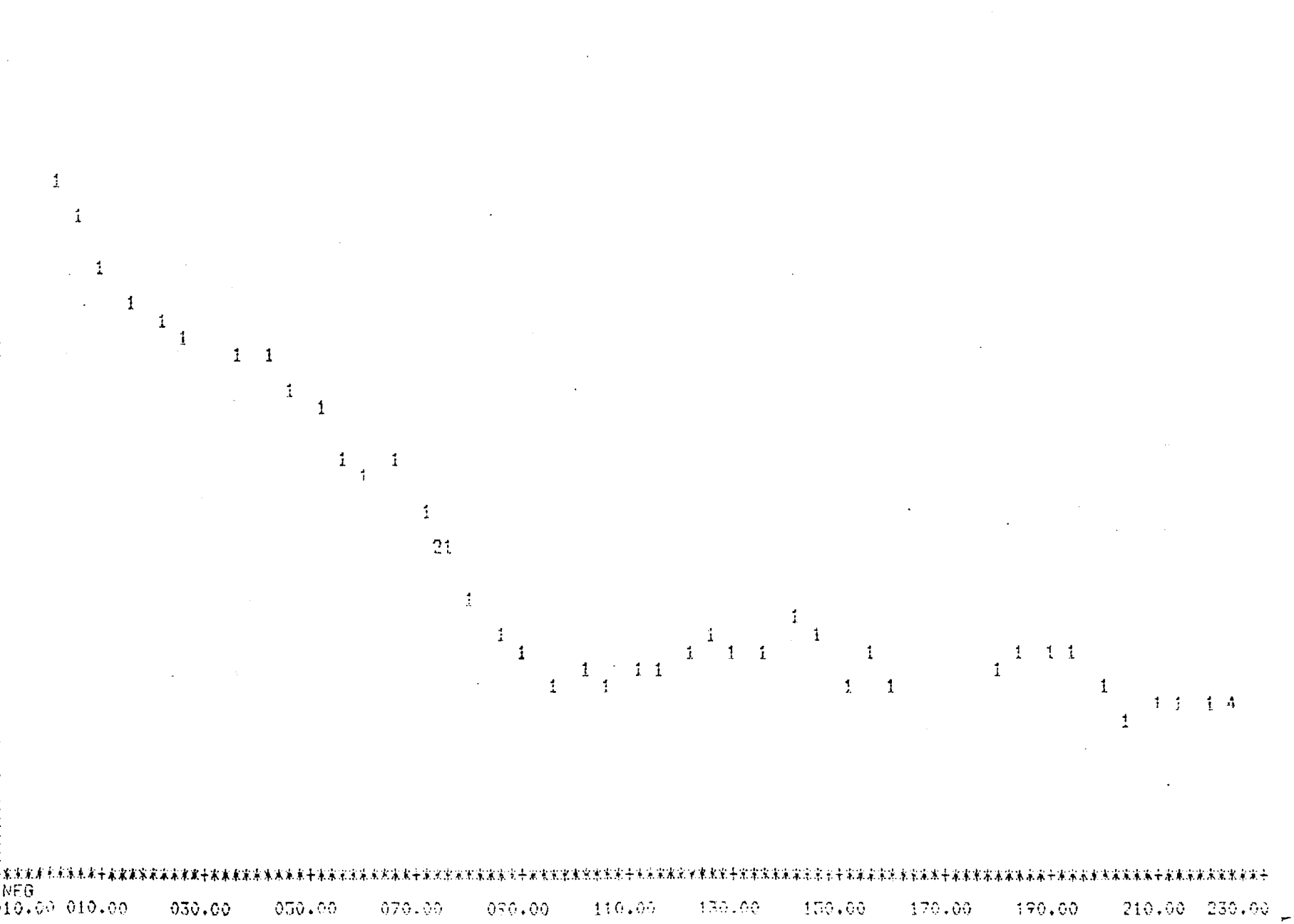

NEG
010.00 010.00 030.00 050.00 070.00 090.00 110.00 130.00 150.00 170.00 190.00 210.00 230.00

Fig. 13

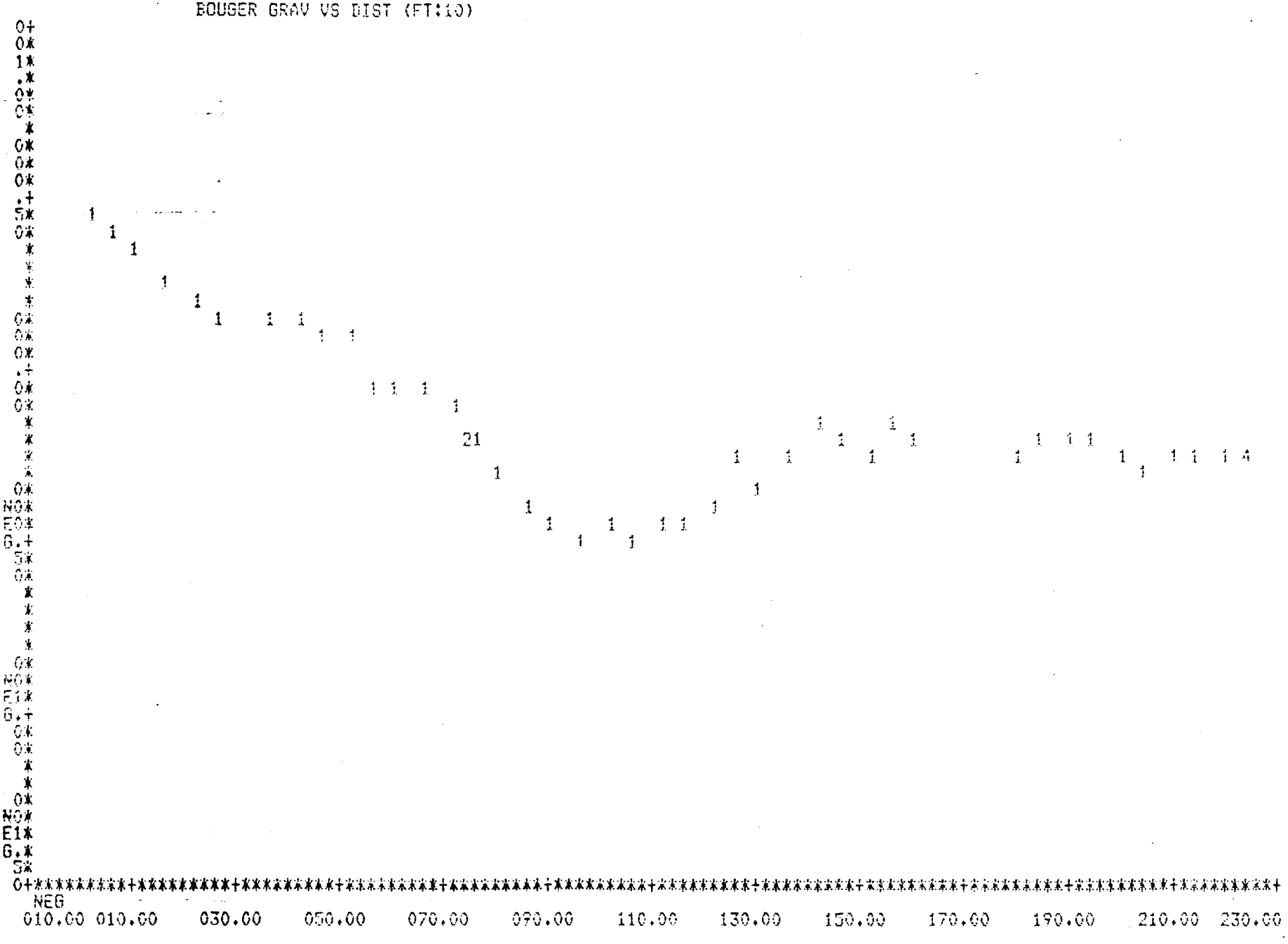

ENTRIES= 47 YUNDER= 0 YOVER= 0 XUNDER= 0 XOVER= 0

DENSITY IS 0.20000000E 01

Fig. 14

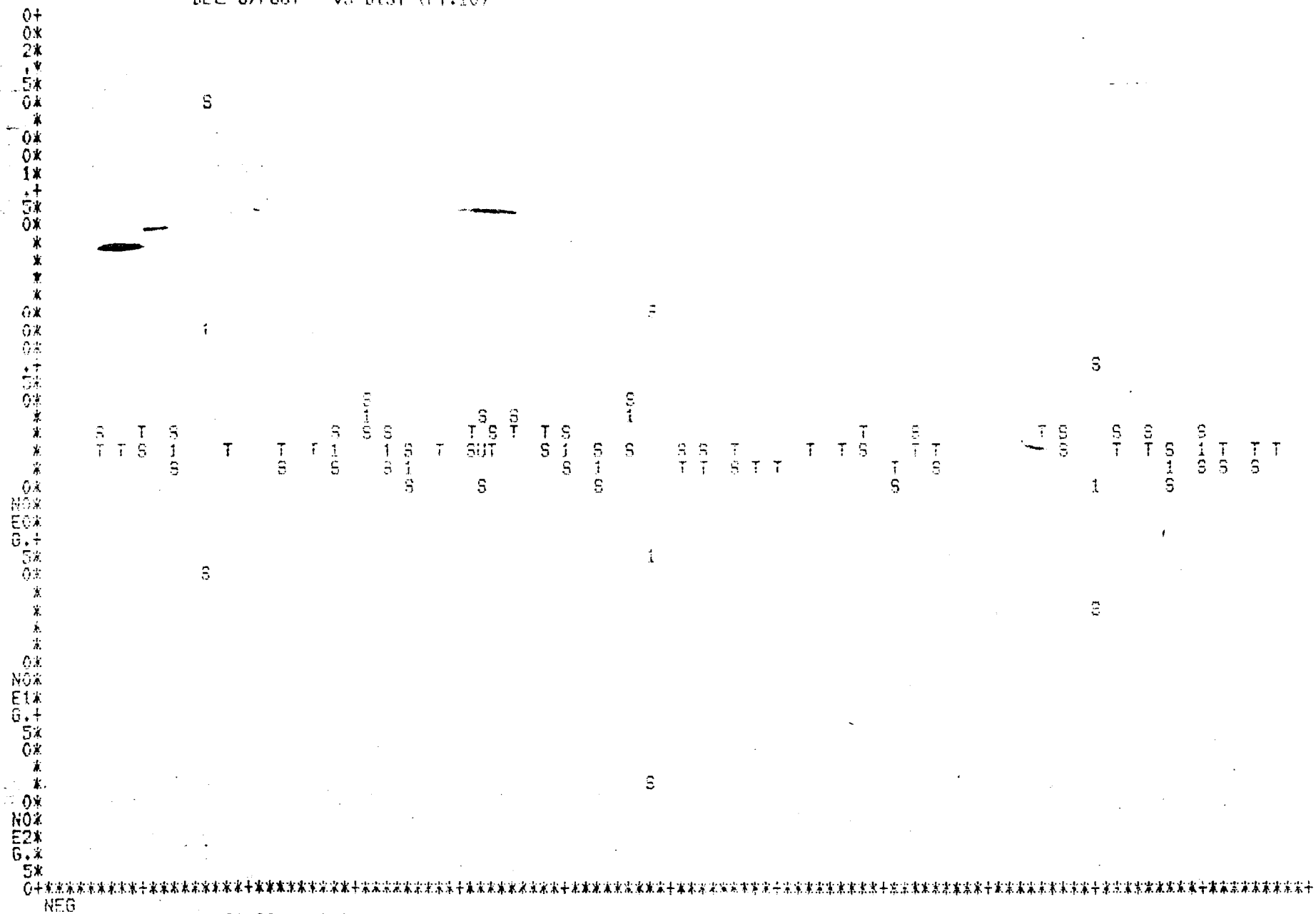
DEL G/FOOT VS DIST (FT:10)
NEG
010.00 010.00 030.00 050.00 070.00 090.00 110.00 130.00 150.00 170.00 190.00 210.00 230.00
ENTRIES= 135 YUNDER= 0 YOVER= 0 XUNDER= 0 XOVER= 0

Fig. 15

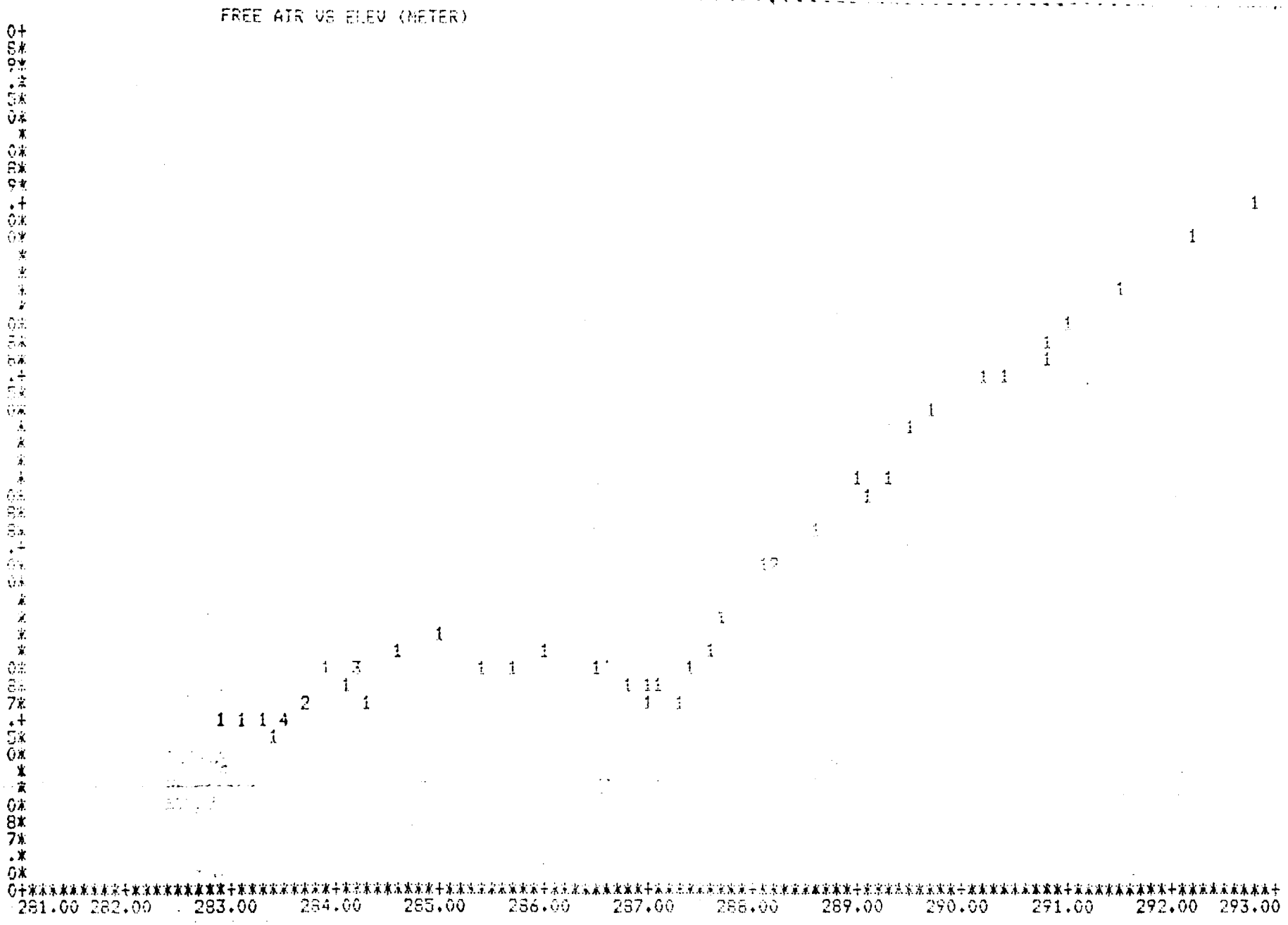

ENTRIES= 47 YUNDER= 0 YOVER= 0 XUNDER= 0 XOVER= 0

Fig. 16

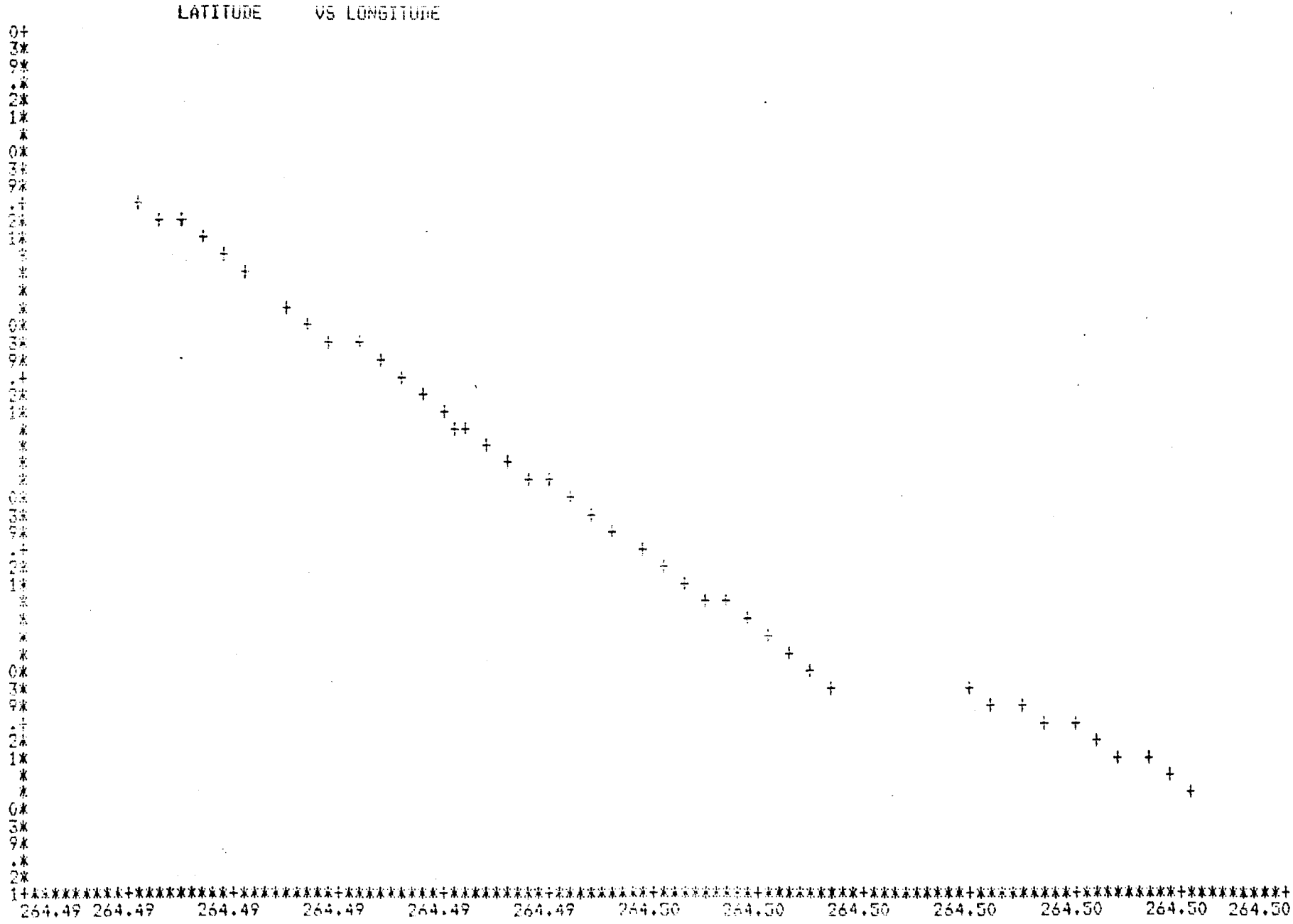
LATITUDE VS LONGITUDE
264.49 264.49 264.49 264.49 264.49 264.49 264.50 264.50 264.50 264.50 264.50 264.50 264.50

Fig. 17

Program REGIONAL

By drawing the location of the profile onto the Bouguer Gravity Map of Northeastern Kansas (Fig. 18) it could be concluded that there might be an increase in the regional gravity from southeast to northwest. Because of the small size of the area, where the data were taken, it is difficult to determine the regional gravity. The conclusion represents only the best possible guess (personal conversation, H. Yarger, 1982). This regional trend is also obvious in the Bouguer plot in Fig. 14 by the general increase in gravity if you go from the right side of the plot to the left. The drop due to the channel is a short wavelength effect, because the source is close to the surface. The regional change is caused by deeper sources and has consequently a longer wavelength. In our case this regional change may be approximated by a linear increase, mainly because the profile is only 2300 ft long. This linear fit of the Bouguer values is done by a least squares fit method:

Linear equation g represents the regional gravity trend

$$g = a + bx$$

The sum over all the square deviations X^2 has to be a minimum.

$$X^2 = \sum_{i=1}^{N} (g_i - x_i)^2$$

where g_i is the Bouguer gravity at the i-th location and x_i is the distance DIST from NWC21.

Now the first derivatives with respect to a and b have to be 0.

$$\frac{dX^2}{db} = \sum_{i=1}^{N} (g_i - a - bx_i)x_i = 0 \qquad \frac{dX^2}{da} = 2\sum_{i=1}^{N} (g_i - a - bx_i)(-1) =$$

$$\sum_{i=1}^{N} g_i x_i - \sum_{i=1}^{N} a x_i - \sum_{i=1}^{N} b x_i^2 = 0 \qquad \sum_{i=1}^{N} g_i = \sum_{i=1}^{N} (a + bx_i)$$

$$\bar{g} = \frac{1}{N}\sum_{i=1}^{N} g_i \qquad \bar{x} = \frac{1}{N}\sum_{i=1}^{N} x_i$$

$$\overline{gx} = \frac{1}{N}\sum_{i=1}^{N}(x_i g_i) \qquad \overline{x^2} = \frac{1}{N}\sum_{i=1}^{N} x_i^2$$

I $\overline{gx} - a\bar{x} - b\overline{x^2} = 0$ II $\bar{g} = a + b\bar{x}$

Solving equation II for a and inserting a into equation I gives:

$$a = \bar{g} - b\bar{x}$$

$$(\bar{g} - b\bar{x})\bar{x} + b\overline{x^2} - \overline{gx} = 0$$

$$b(\overline{x^2} - (\bar{x})^2) = \overline{gx} - \bar{g}\bar{x}$$

$$b = \frac{\overline{gx} - \bar{g}\bar{x}}{\overline{x^2} - (\bar{x})^2}$$

$$a = \bar{g} - \frac{\overline{gx} - \bar{g}\bar{x}}{\overline{x^2} - (\bar{x})^2}\,\bar{x}$$

The result can be seen in Fig. 19 where the Bouguer gravity together with the linear regional approximation are plotted. It was important for this least squares fit to avoid multiple contributions of stations. That means that the overlap station RTH (Resistivity Test Hole) and the base station SES10 were only counted once.

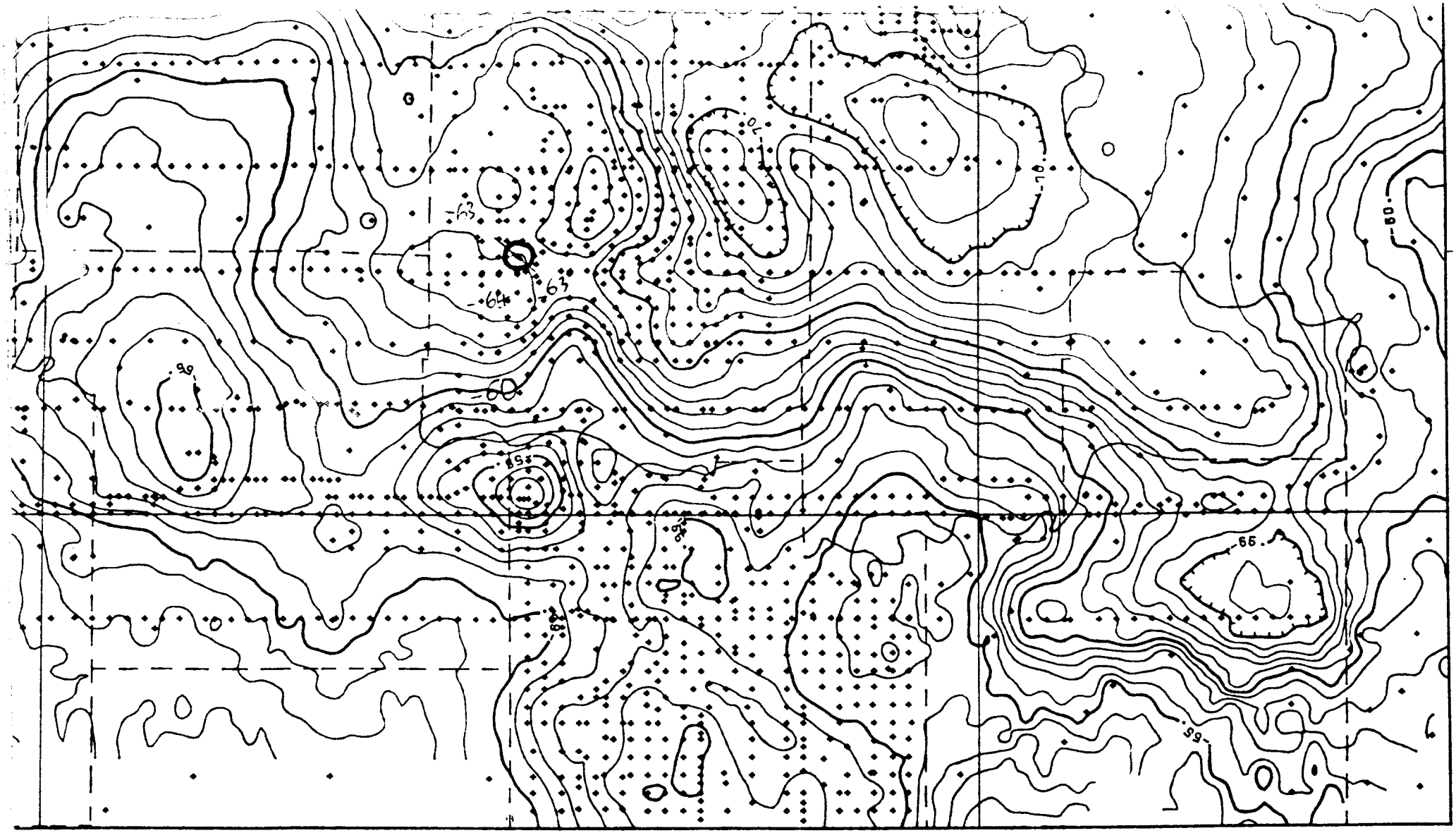

96.0

264

95.0

265

longitude

orientation of profile

real profile is much smaller

Scale: 1:500,000

1 inch equals approximately 8 miles

10 0 10 20 30 40 Miles

Fig. 18

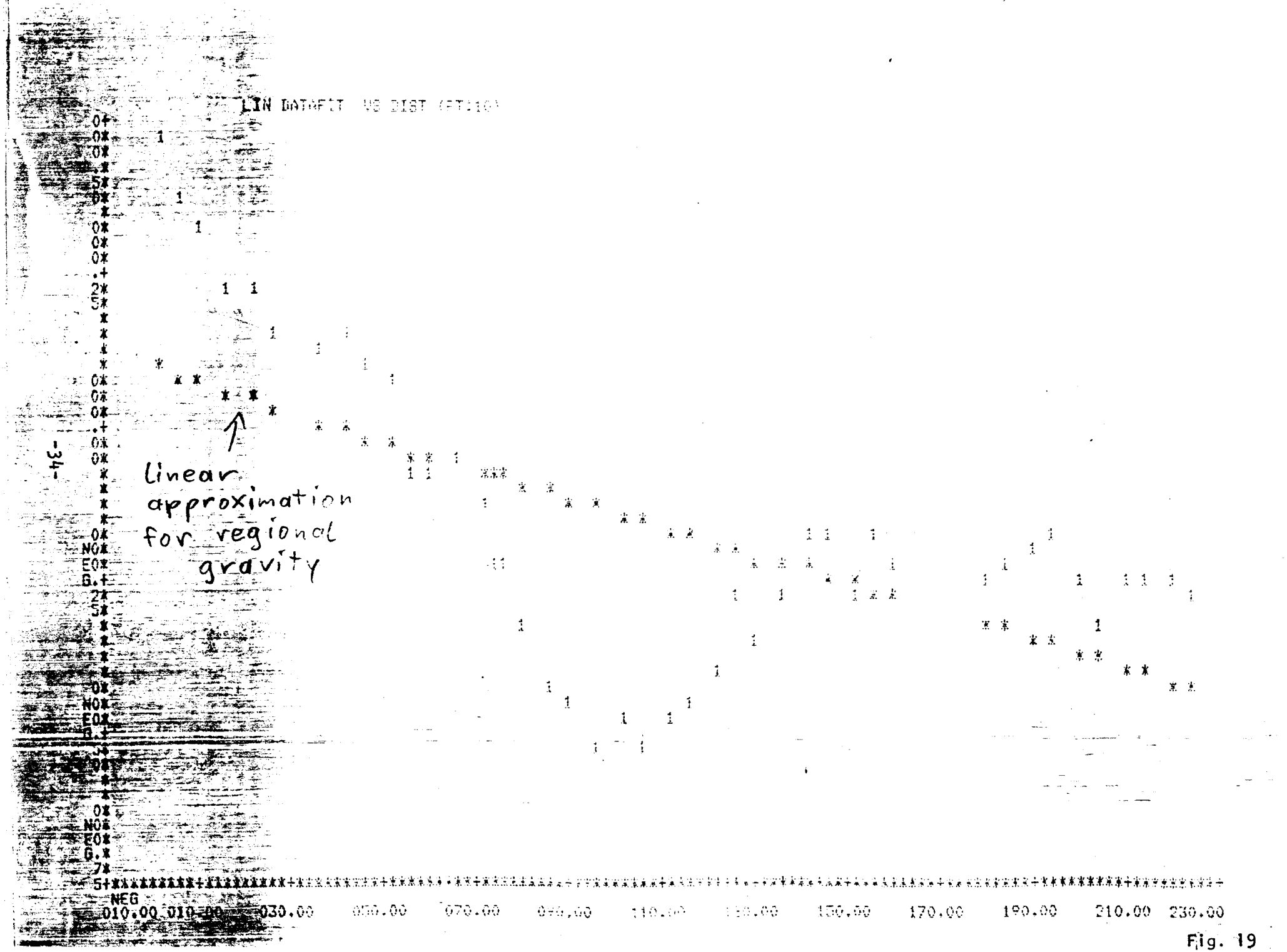
LIN BATHFIT VS DIST (FT)(0)
linear approximation for regional gravity
NEG
010.00
030.00
070.00
110.00
150.00
170.00
190.00
210.00
230.00

Fig. 19

Residual gravity vs dist (ft/10)

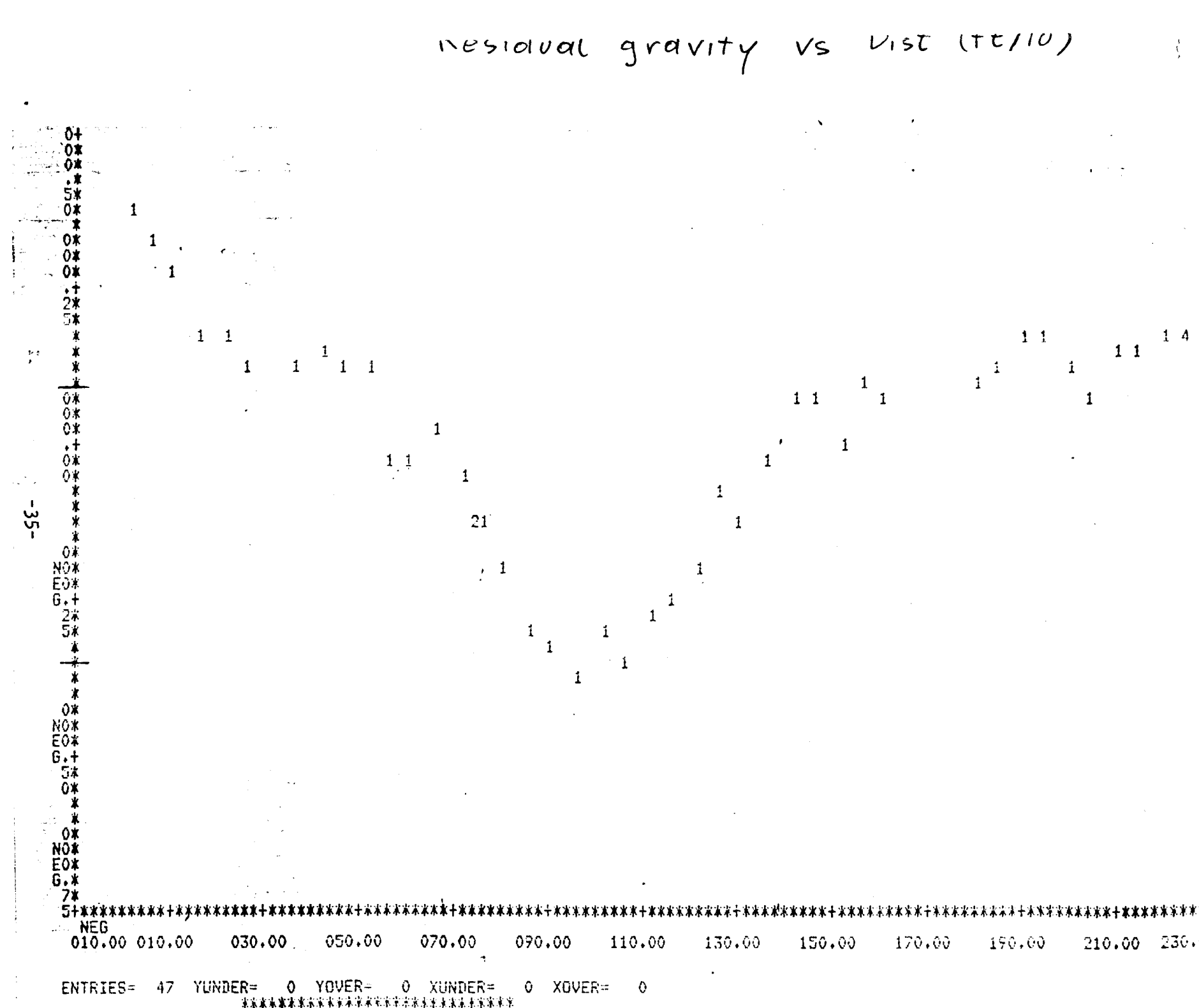

ENTRIES= 47 YUNDER= 0 YOVER= 0 XUNDER= 0 XOVER= 0

DENSITY IS 2.

Fig. 20

Program RESIDUAL

The program calculates the residual gravity values by subtracting the linear approximated regional gravity from the Bouguer gravity. The result is plotted versus distance and can be seen in Fig. 20. The anomaly in gravity is approximately 0.45 mgal. This residual gravity is the final result after all the reductions. It should be closely correlated to changes in the bedrock topography. Estimating the bedrock topography is done in the final step, the modeling.

Modeling Program PRISM

The cumulative gravity effect from prisms of different sizes and density contrasts is matched to the residual gravity graph as closely as possible. The density contrast is negative, because the bedrock density is higher than the density of the valley fill material. The closer the prisms are to the surface, the higher is their contribution to the modeled response. The more negative the density contrast, the bigger is the drop in gravity. A small prism close to the surface might have the same anomaly that a bigger one that is deeper would have. Thus, there is no unique solution for obtaining one certain model result.

By establishing boundary conditions, the range of possibilities can be diminished. Practically, that means bedrock depth information should be obtained from drillholes. These drillholes allow only a certain range of prism sizes to be used. In our case, two points of the valley are fixed by the drillholes RTH and C which hit bedrock at 49 ft and 142 ft. There is a maximum number of 19 prisms available in this program PRISM. It is important that the slope of the Bouguer gravity data and the slope of the modeled gravity are in good accordance.

Upper Pennsylvanian (continued)		Calhoun Shale		20-45 30	Gray to brown silty to sandy shale, locally containing silty fine-grained sandstone.
Virgilian (continued)	Shawnee (continued)	Deer Creek Limestone	Ervine Creek Limestone	30-40 35	Upper limestone is thick bedded with wavy partings and gray weathering to yellowish brown. Upper shale unit grades upwards from black fissile shale to light-gray silty and sandy shale. Middle limestone is gray to brown weathering to yellowish brown. Lower shale is calcareous, clayey, and gray to brown weathering yellowish brown. Lower limestone is thick bedded with shale partings and brownish gray weathering to yellow brown.
			Undifferentiated Burroak and Larsh Shale		
			Rock Bluff Limestone		
			Oskaloosa Shale		
			Ozawkie Limestone		
		Tecumseh Shale		60-85 70	Bluish-gray to olive-gray silty to sandy shale locally containing silty fine-grained sandstone beds.
		Lecompton Limestone	Avoca Limestone	30-45 40	Upper limestone is dark gray weathering to light yellowish brown and is interbedded with gray silty shale. Upper shale is clayey and olive gray weathering to gray. Second limestone is thin to medium bedded, bluish gray weathering to light tan, and very fossiliferous; contains interbeds or partings of shale. Middle shale grades upward from black carbonaceous shale to gray clayey shale. Third limestone is dense and bluish gray weathering to light brownish gray. Lower shale is clayey and dark gray weathering light yellowish brown or light gray; contains some shaly limestone beds. Lower limestone is dark gray weathering to brown.
			King Hill Shale		
			Beil Limestone		
			Queen Hill Shale		
			Big Springs Limestone		
			Doniphan Shale		
			Spring Branch Limestone		
		Kanwaka Shale	Stull Shale	60-90 90	Upper shale is dark gray and silty to sandy; locally contains a silty fine-grained sandstone. Limestone is thin, dense, and bluish gray weathering to light grayish brown. Lower shale is silty to sandy and bluish gray; locally contains a silty fine-grained sandstone.
			Clay Creek Limestone		
			Jackson Park Shale		

chosen values for thickness

(after Jewett, J. D. Hinrichs, 1942)

Fig 21

Density Determination

The density contrast between bedrock and valley fill material is obtained from information about thickness and density of the different bedrock layers.

The density of certain layers can be calculated from the seismic velocities of sound waves and the use of a conversion graph which assigns to every velocity a certain density (Fig. 23). Using available seismic data, this proves for this purpose rather inaccurate, because of the wide velocity range for each individual layer and therefore gives a wide density range. The reason for this wide range is, that the seismic measurements are valid for Jefferson and Nemaha County (Denne and others, 1982). A better approach is the use of a compensated neutron-formation density log (on file with the State Geological Survey) which allows determination of the density with accuracy to 1/100 g/cm^3 (personal communication with Lynn Watney, 1982).

The log used was taken by Trans Ocean Oil, Inc., in Wabaunsee county, Kansas in 1975. It was in section 27, township 10S and range 11E. The densities of the Deer Creek Limestone and the Lecompton Limestone were obtained by taking the average densities of the formation members. The density values are:

Calhoun Shale	2.43 g/cm^3
Deer Creek Limestone	2.51 g/cm^3
Tecumseh Shale	2.46 g/cm^3
Lecompton Limestone	2.51 g/cm^3

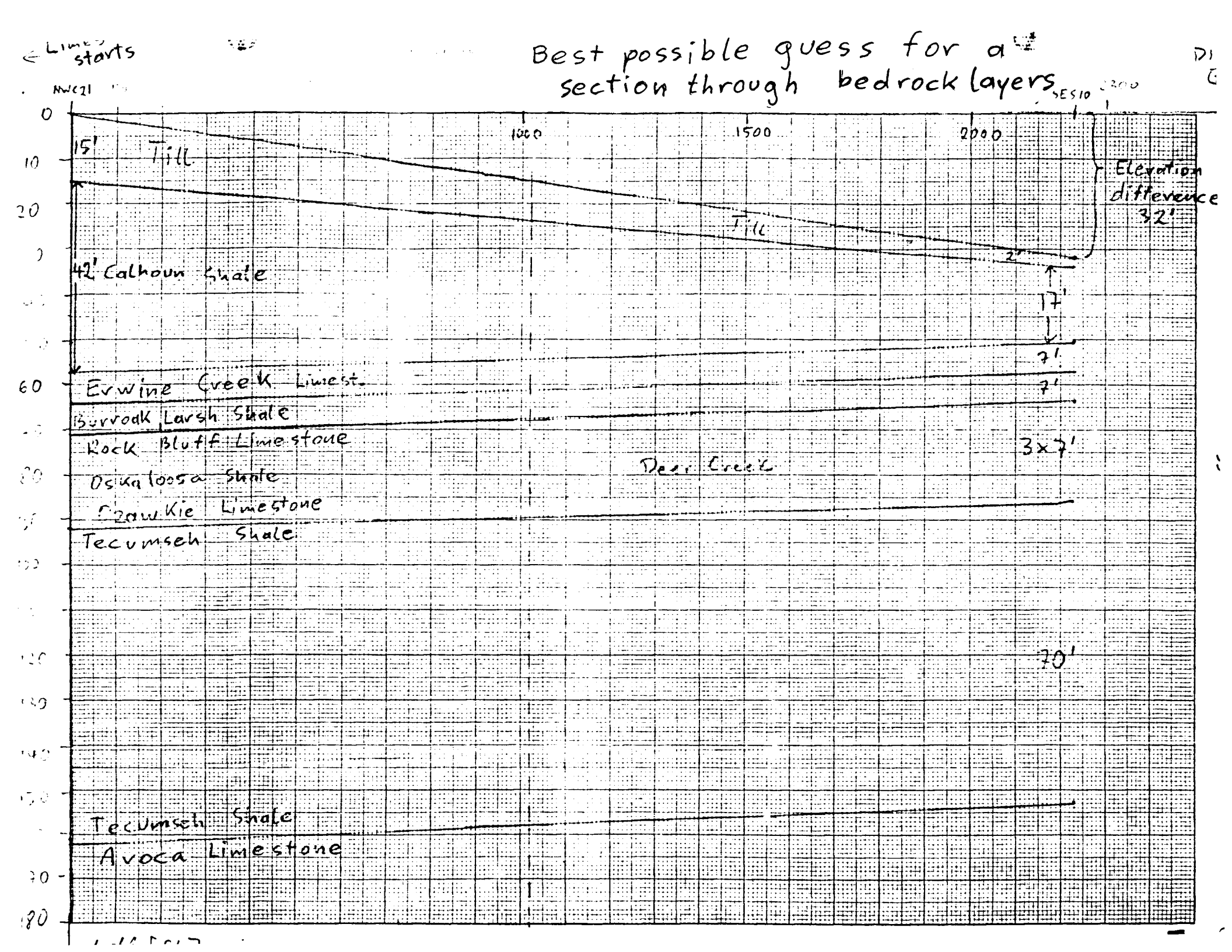
Best possible guess for a section through bedrock layers
Lime starts
NW 21
SE 10
0
10
20
60
80
120
140
160
180
1000
1500
2000
15' Till
Till
42' Calhoun Shale
Erwine Creek Limest.
Burroak Larsh Shale
Rock Bluff Limestone
Oskaloosa Shale
Rawkie Limestone
Tecumseh Shale
Deer Creek
Tecumseh Shale
Avoca Limestone
Elevation difference 32'
2'
17'
7'
7'
7'
3x7'
70'

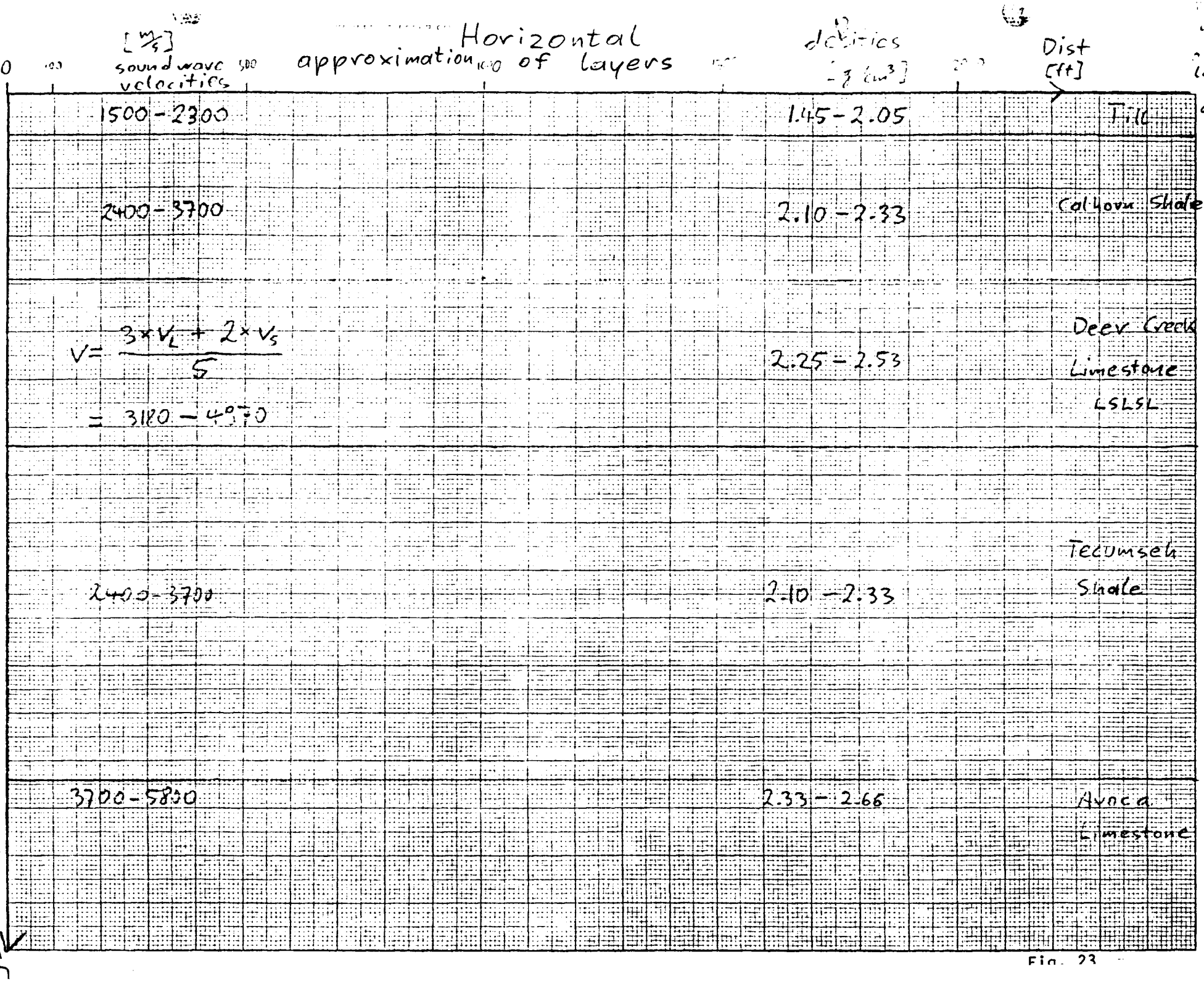
Horizontal approximation of layers
[m/s] sound wave velocities
densities [g/cm³]
Dist [ft]
0
1500-2300
1.45-2.05
Till
9
2400-3700
2.10-2.33
Calhoun Shale
39
$V = \frac{3 \times V_L + 2 \times V_S}{5}$
= 3180 - 4070
2.25-2.53
Deer Creek Limestone
LSLSL
74
-40-
Tecumseh Shale
2400-3700
2.10-2.33
144
3700-5830
2.33-2.66
Avon a Limestone
depth [ft]

Fig. 23

Although the log was not taken at the profile location, it is assumed there is not much density change within the same layer. The fixed densities of the bedrock layers leave the fill material density ρ_{Fill} as a parameter, whose range can be chosen from seismic-and well data.

Thickness of Formation

With the use of Fig. 21, thicknesses of the individual layers were estimated. This table comes from the report "Geohydrology of Jefferson County" (Winslow, 1972). From the well log of RTH it is known that bedrock occurs at a depth of 49 feet. Rock units include gray and tan clay (shale), a thin limestone layer, and black organic shale. This description corresponds best with the Larsh and Burroak Shale, which are members of the Deer Creek Limestone formation. The units are described in "The Stratigraphic Succession in Kansas" by D. Zeller (1968).

From Fig. 22, the thickness of the Calhoun Shale was estimated to be 33 feet. The Calhoun Shale is a subcrop, which is covered by Till. The thickness of the Till diminishes from an estimated 15 feet in the NW to approximately 2 feet in the SE. (Personal communication, Jane Denne, 1982). The general trend of the formations in the profile is a slight dip by 6 ft over the profile length of 2300 ft towards the west (calculated from information in Winslow (1972)).

The well log of drill hole C shows the first bedrock at a depth of 142 ft. First it is white limestone, and between 147 feet and 150 ft it is gray limestone. As a best guess, this is assumed to be the Avoca Limestone in the Lecompton Limestone formation. "The Avoca Limestone

Member is a dark bluish-gray, somewhat earthy Limestone," and it ranges from 1 to 20 feet in thickness (Zeller, 1968). A less likely alternative to the Avoca Limestone is the Spring Branch Limestone in the Lecompton Limestone. The Spring Branch Limestone is a gray somewhat sandy limestone, generally about 4 ft thick (Zeller, 1968). This information and consideration of a surface slope of 32 feet towards SE gives Fig. 22.

The water well records within the same section were not very useful for bedrock data and therefore generalized thicknesses were chosen. In summary, the model is hypothetical. The rock units are not critical for the final result, because all have a density between 2.4 g/cm^3 and 2.5 g/cm^3.

Mapping the Formations

For the modeling process all the dips shown in Fig. 22 are considered neglible. All the layer thicknesses are averaged to the thickness they have under the minimum of the gravity anomaly which is at DIST 1000 ft. That means the layers are assumed to be horizontal as shown in Fig. 23. Also, from the well logs one determines a density range for the fill material. It is mainly sand and gravel, which leads to a possible range from 1.7 to 2.3 g/cm^3. (Personal communication, Lynn Watney, 1982). All this information is combined to yield Fig. 25 and 26, which show the two main results of the modeling. For a certain fill material density ρ_{Fill}, the density contrasts are fixed and the only variable is the size of the prisms. The size is still restricted by the condition that the walls or bottom of the valley have to touch the points where the drillholes hit bedrock.

A typical input of data for the modeling program looks like Fig. 24:

	WEST	EAST	TOP	BOTTOM	DENS
1	530.0	1600.0	7.00	16.00	-0.33
2	580.0	1550.0	16.00	24.00	-0.33
3	650.0	1500.0	24.00	39.00	-0.33
4	700.0	1480.0	39.00	56.00	-0.41
5	730.0	1200.0	56.00	74.00	-0.41
6	790.0	1160.0	74.00	104.00	-0.36
7	530.0	1150.0	104.00	124.00	-0.36
8	560.0	1110.0	124.00	144.00	-0.36
9	950.0	1050.0	144.00	170.00	-0.41

West: Western edge of the prism

East: Eastern edge of the prism

Top: Depth at which prism starts

Bottom: Depth at which prism ends

Dens: Density contrast between bedrock and valley fill material

Results of the Modeling

The following results were obtained after trying many different prism sizes and density contrasts. The best fits were in the range from 2.10 g/cm^3 to 2.20 g/cm^3. These values are considered the acceptable minimum and maximum fill material densities.

A good correlation between the slopes of the gravity data and the modelled profile is important. The model data have to fit the minimum gravity data (bottom of anomaly), because this determines the depth of the valley. The curvature of the gravity data had to be fit, in order to determine the shape of the valley. A good fit was accomplished by considering NWC 10 and NWC 11 as noisy data. The fit was not obtained by a mathematical method, but by best guessing.

Looking now at different examples:

$\rho_{Fill} = 2.09$ g/cm^3 (Fig. 25)

There is a good fit possible, but the modeled gravity deviates from the Bouguer gravity at the right bottom of the valley. This is because the prisms are forced to have a certain width between 124 and 150 ft to fulfill the requirement of testhole C. Therefore, 2.09 is not accepted as a good fill density.

$\rho_{Fill} = 2.10$ g/cm^3 (Fig. 26)

Going to the next higher fill density the modulus of the density contrast becomes smaller, because density contrast is defined as:

$$\Delta\rho = \rho_{Fill} - \rho_{Layer}$$

So even with the comparatively wide prisms at the valley bottom we get a very good fit. In this case the valley has the smallest possible depth and volume, which is the lower size limit from the modeling, and which has the highest density contrast modulus that is acceptable. It is also the most probable valley form because there is a bigger chance that erosion ends above limestone than above or in shale. In the general area of northeastern Kansas the seismic data suggest a lower fill density than 2.10 g/cm^3 (Denne and others, 1982). Another support for this case is the fact that C may be close to the bottom of the valley. C hits bedrock at 142 ft. The maximum known valley depth in this area is 167 feet. This is based on another drillhole several hundred feet south of RTH.

Another important point is that the slopes of the Bouguer graph are in accordance with the modeled graph. The points NWC10 and NWC11 represent noise or a small change in bedrock topography which is not modeled.

$\rho_{Fill} = 2.20$ g/cm^3 (Fig. 27)

At the high fill density the modulus of the density contrast becomes quite small and therefore you have to go to greater depth in order to get the same gravity effect. Again the drillholes and RTH pose boundary conditions. The slope of the valley walls is still acceptable. The valley is now 260 ft deep and has its highest acceptable volume for the modeling. Notice, that it still follows the slopes, even at the left side of the profile. That this fill density is the highest possible one can be seen from the next two cases.

$\rho_{Fill} = 2.21\ g/cm^3$ (Fig. 28)

For this case, the valley has to be 290 feet deep to get a fit that drops deep enough in order to reach the lowest data points. If you consider the data NWC10 and NWC11 as noise, you find a common slope for the Bouguer data at the left side of the valley. The modeled gravity gradient visibly deviates from the measured slope.

$\rho_{Fill} = 2.22\ g/cm^3$ (Eig. 29)

By using a 310 feet deep valley the modeled profile fits more or less all the data in magnitude, but the slope at the left side of the buried valley deviates even more than in Fig. 28.

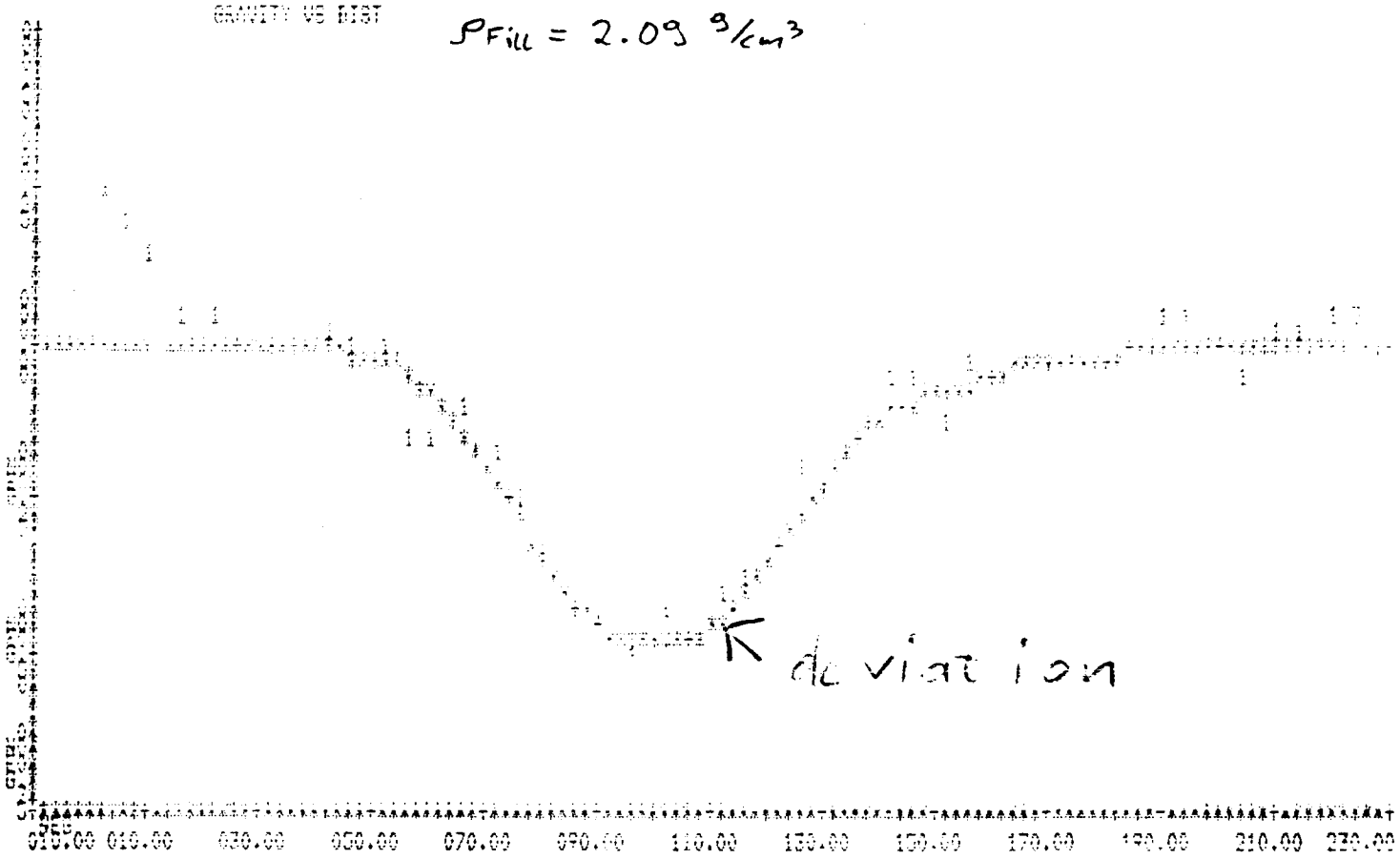
GRAVITY VS DIST
$\rho_{Fill} = 2.09\ g/cm^3$
deviation
010.00
030.00
050.00
070.00
090.00
110.00
130.00
150.00
170.00
190.00
210.00
230.00

Fig. 25

Bouguer gravity and buried valley cross section

(valley fill density ρ_{Fill} = 2.10 g/cm^3)

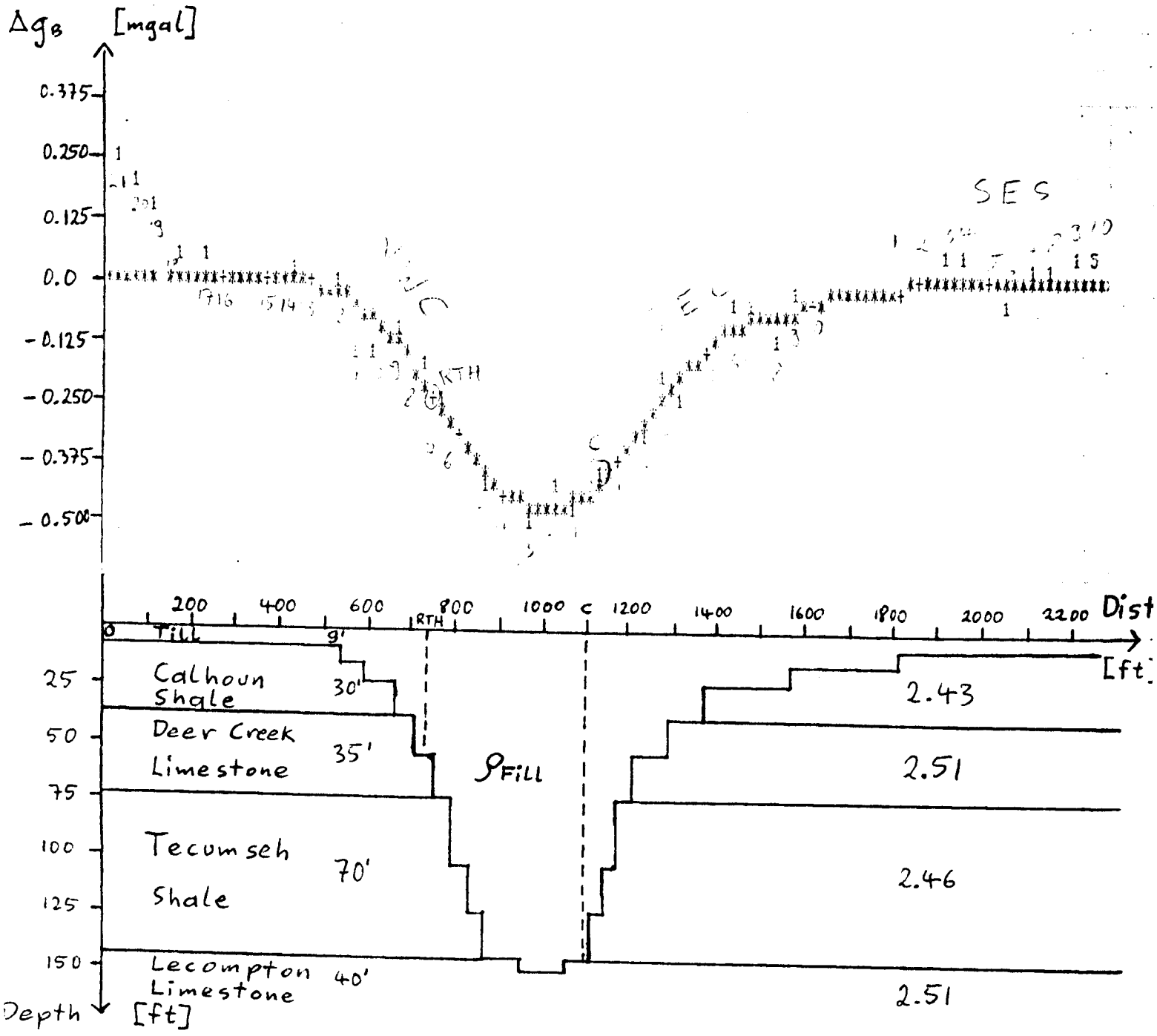

Formation or rock unit	Thickness in feet	Formation density in g/cm^3

Fig. 26

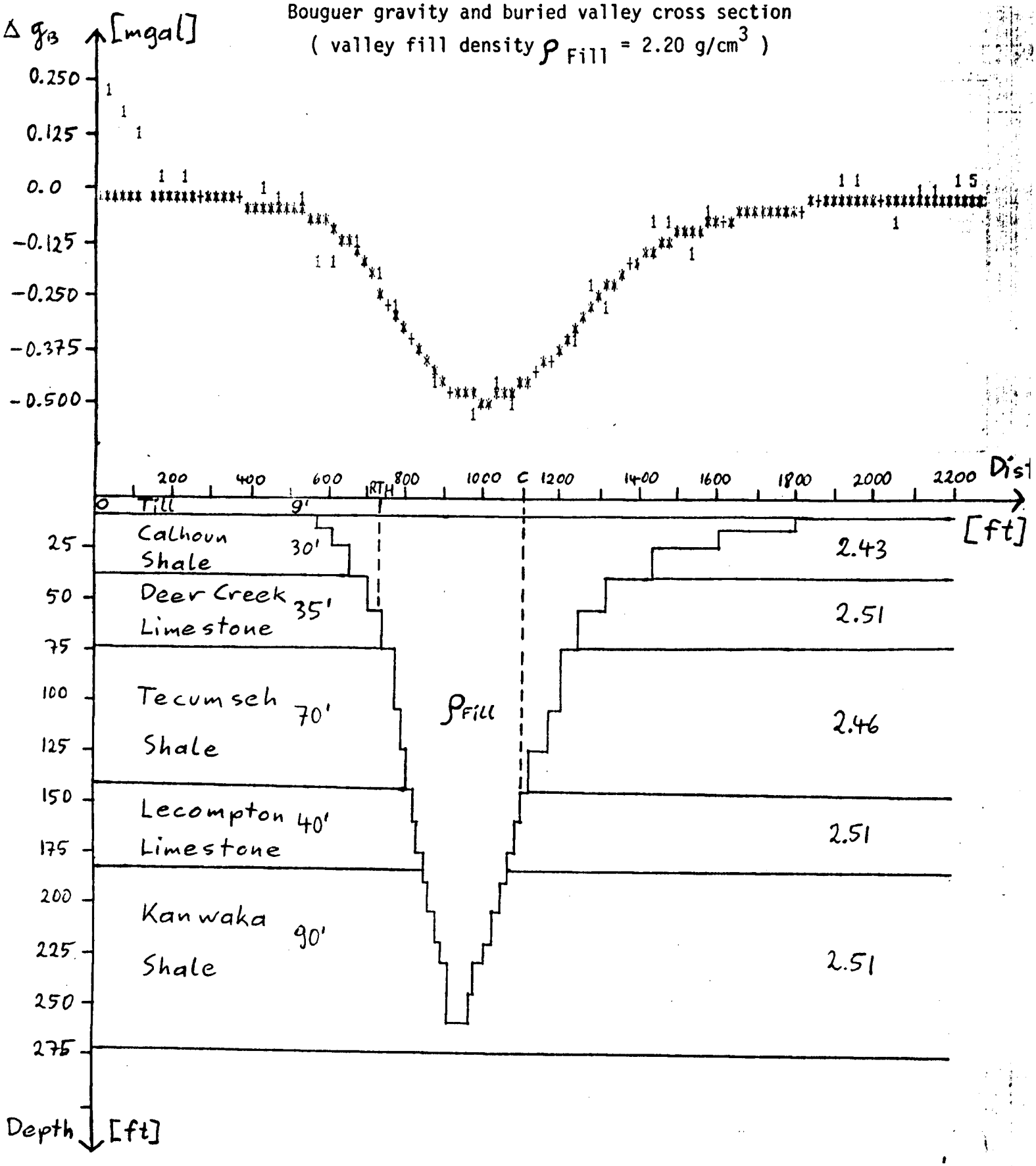

Formation or rock unit	Thickness in feet	Formation density in g/cm^3

Fig. 27

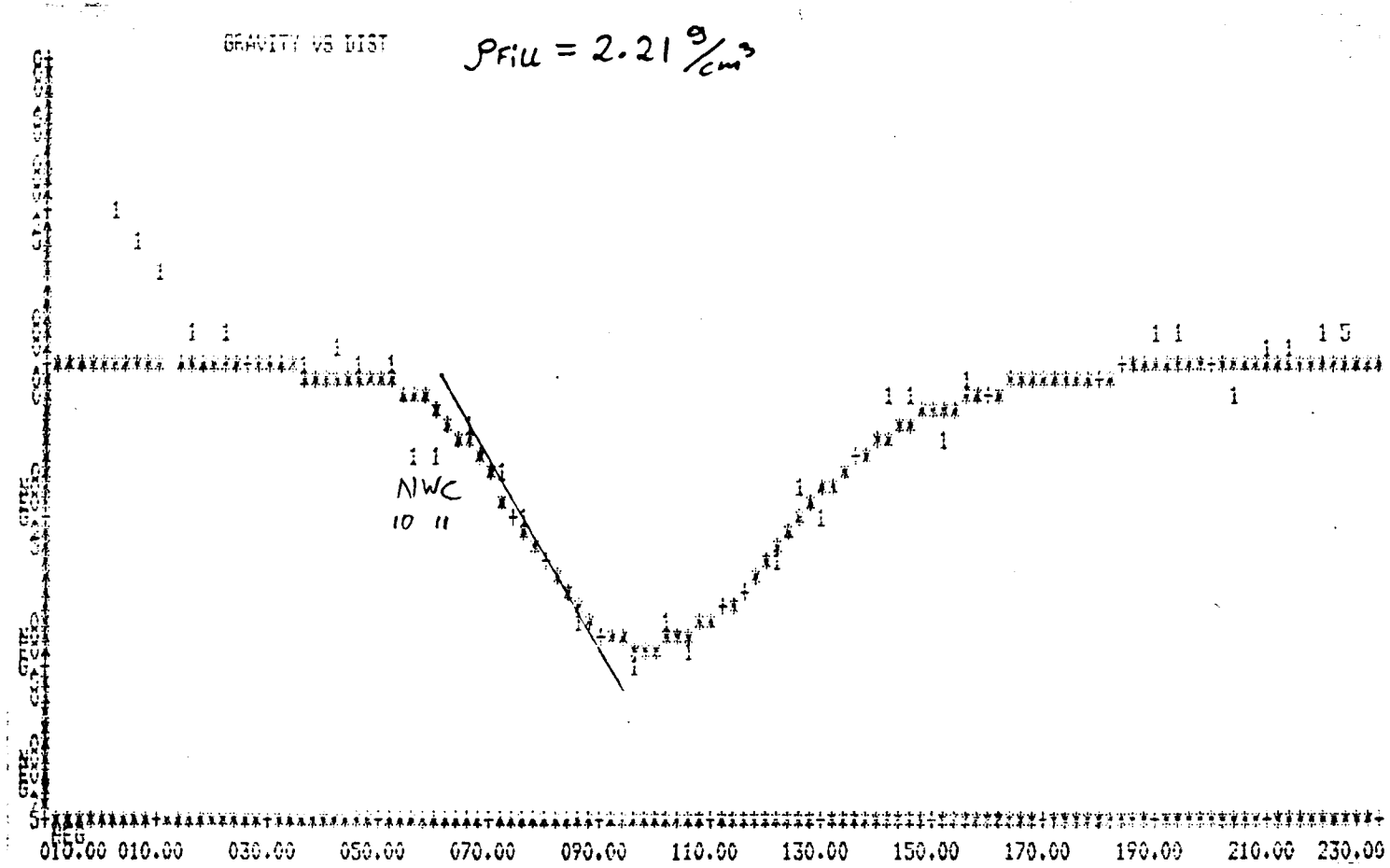

depth of valley: 290 ft

Fig. 28

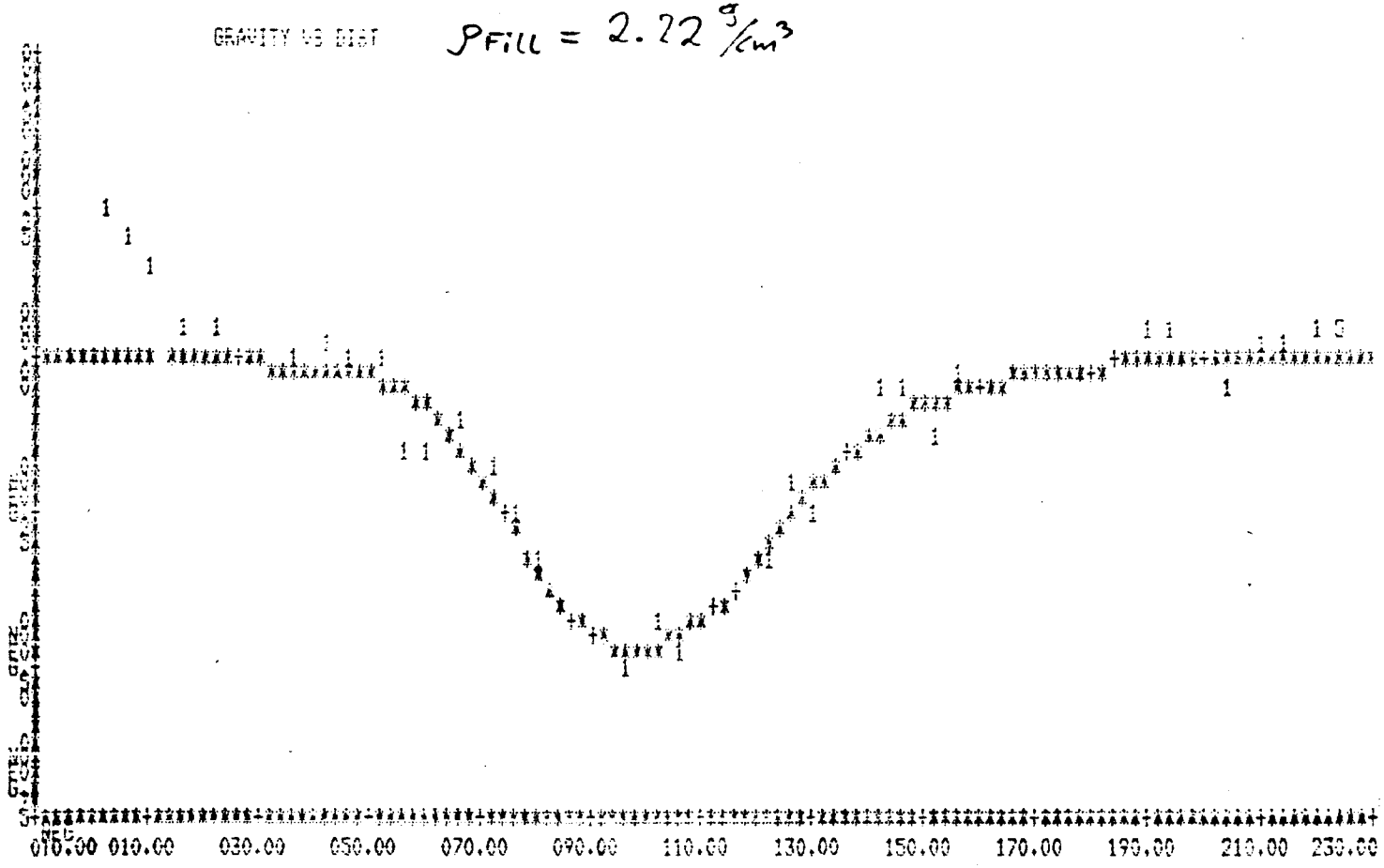

dept of valley: 310 ft

Fig. 29

Conclusions

There are two main conclusions from this research.

First, it tests the gravity method over a buried channel. The gravity method proves to be a useful tool in detecting buried channels. Second, the good control through the wells pins down the density of the fill material to a range of 2.10 g/cm^3 to 2.20 g/cm^3. This again determines a minimum and maximum size of the valley. The minimum depth is 150 feet and the maximum depth is 260 feet.

The method can be applied to locate ground water resources associated with the buried valleys. Because of the modest size of the gravity anomaly, care must be taken in taking the gravity data and in measuring the elevation. In future research it could be found out how much the sensitivity of this method can be improved by the use of more exact elevation and gravity measurements. It would be interesting to find the smallest size of valleys that could be detected by the gravity method. With more drillholes available the method could be improved. More drillholes could increase the accuracy in the determination of the thickness of the rock units. After the first Bouguer profile over a suspected buried channel was obtained, drillholes should be made at the assumed walls and the bottom of the valley to set more boundary conditions for the modeling of the valley. Drillholes also will give an evaluation of water availability.

In combination with drillholes, the gravity method is a easier, quicker and cheaper method than drilling alone.

Acknowledgments

The author wishes to express his appreciation to Jane Denne, Dr. Carl McElwee and Dr. Harold Yarger for their guidance and suggestions. Special thanks also go to the students George Lam, Allen Martin and Rita Sooby who advised me in working with the computer and changing the programs.

Bibliography

Carmichael, R.S. and Henry, G., Gravity exploration for groundwater and bedrock topography in glaciated areas; Geophysics, Vol. 42, No. 4 (June 1977), p. 850-859.

Denne J., Steeples D., Sophocleous M., Severini, A. and Lucas, J., An integrated approach for locating glacial buried valley aquifers; KGS Groundwater series No. 5, 1982, in press.

Griffiths, D. and King R., Applied Geophysics Pergamon International Library, 1976, p. 143 F.

Hall, H. and Hajnal, Z., The gravimeter in studies of buried valleys, Geophysics, Vol. 27, 1962, p. 931-951.

Hammer, S.V., Terrain corrections for gravimeter stations, Geophysics, 4, pp. 184-194.

Ibrahim, A. and Hinze, W., Mapping buried bedrock topography with gravity, Groundwater, Vol. 10, No. 3, May-June 1972.

Winslow, J., Geohydrology of Jefferson County, KGS Bulletin 202, part 4, 1972.

Zeller, D., The stratigraphic succession in Kansas; KGS, Bulletin 189, 1968.